Sikalo, Nejra; Hasemann, Olaf; Schulz, Christof; Kempf, Andreas; Wlokas, Irenäus:

A Genetic Algorithm-Based Method for the Optimization of Reduced Kinetics Mechanisms

DOI: http://dx.doi.org/10.1002/kin.20942

URN: urn:nbn:de:hbz:464-20170504-153534-9

Link: https://duepublico.uni-duisburg-essen.de:443/servlets/DocumentServlet?id=42267

Source: International Journal of Chemical Kinetics, 47: 695–723 (2015); First published: 23 September 2015

A Genetic Algorithm-Based Method for the Optimization of Reduced Kinetics Mechanisms

N. Sikalo[1]*, O. Hasemann[1], C. Schulz[2, 3], A. Kempf[1, 3, 4], I. Wlokas[1]

[1] Chair of Fluid Dynamics – IVG, Institute for Combustion and Gas Dynamics
[2] Chair of Reactive Fluids – IVG, Institute for Combustion and Gas Dynamics
[3] CENIDE, Center for Nanointegration Duisburg-Essen
[4] CCSS, Center for Computational Sciences and Simulation

University of Duisburg-Essen, 47048 Duisburg, Germany

Note: This document is an authors' version of the manuscript that was accepted for publication in International Journal of Chemical Kinetics. Changes made during the publishing process, such as peer review, editing, corrections, structural formatting, and other quality control mechanisms may not be reflected in this document. Please cite the original publication as:

Sikalo, N., Hasemann, O., Schulz, C., Kempf, A. and Wlokas, I. (2015), A Genetic Algorithm–Based Method for the Optimization of Reduced Kinetics Mechanisms. Int. J. Chem. Kinet., 47: 695–723. doi:10.1002/kin.20942

Abstract

This paper describes an automatic method for the optimization of reaction rate constants of reduced reaction mechanisms. The optimization technique is based on a genetic algorithm that aims at finding new reaction rate coefficients that minimize the error introduced by the preceding reduction process. The error is defined by an objective function that covers regions of interest where the reduced mechanism may deviate from the original mechanism. The mechanism's performance is assessed for homogeneous-reactor or laminar-flame simulations against the results obtained from a given reference – the original mechanism, another detailed mechanism, or experimental data, if available. The overall objective function directs the search towards more accurate reduced mechanisms that are valid for a given set of operating conditions. Part of the objective function is a penalty term that helps to minimize the change to the reaction coefficients, keeping them as close as possible to the original value. It is demonstrated that the penalty function is successful and can be combined with predefined uncertainty bounds for each reaction of the mechanism. In addition, the penalty function can be modified to achieve a further reduction of the mechanism. The algorithm is demonstrated for the optimization of a previously reduced variant of GRI-Mech 3.0, a *tert*-butanol combustion mechanism provided by Sarathy et al. (2012) and a hydrogen mechanism by Konnov (2008), for which the complete uncertainty vector is known. The method has

shown to be robust, flexible, and suitable for a wide range of operating conditions by using multiple criteria simultaneously.

Keywords: Reaction Mechanisms, Optimization, Genetic Algorithm, Reduction

1. Introduction

Although the detailed description of complex kinetics provides accurate results, its application to the simulation of practical flames in more than one dimension is strongly limited by the available computational resources. In these cases, simplified mechanisms must be used instead. There is a trade-off between the level of simplification, the quality of prediction, the faithfulness to the original mechanism and the range of conditions over which the simplified mechanism is valid. This paper provides a strategy for optimizing reduced mechanisms to achieve the best, case-specific trade-off in the criteria mentioned above. Together with our previous work on the reduction of mechanisms [1], the new method provides an easy-to-use set of tools for the flexible optimization/reduction of mechanisms as the basis of detailed simulations of complex combustion problems.

Various methods have been proposed for the reduction of reactions mechanisms [2, 3]. The reduction approaches can generally be divided into skeletal reduction [4-12], lumping of species or reactions [13-17], and methods based on time-scale analysis [18-22]. Skeletal reduction methods detect and eliminate unimportant species or reactions using sensitivity analysis [4], directed relation graph analysis [8, 9], or flux analysis [10-12]. Lumping approaches group the species according to their similarities in terms of their thermal and transport properties (e.g., isomers), thus reducing the number of species. Methods based on time-scale analysis identify and decouple fast and slow reactions, which results in algebraic equations that couple quasi-steady-state species and partial equilibrium reactions.

Reduction aims at making the mechanisms less costly to solve, albeit with a somewhat lower accuracy. In order to keep the mechanism computationally inexpensive and to enhance its prediction ability, optimization approaches have been developed. Where a reduction can remove entire reactions, optimization must subtly adjust the kinetics coefficients of the elementary reactions to improve the overall agreement with either experimental data or the results from a detailed mechanism.

The kinetics of each elementary reaction in the mechanisms are usually described by three coefficients, the pre-exponential factor A_i, the temperature exponent β_i, and the activation energy $E_{a,i}$. These coefficients are available from experimental databases, theoretical calculations, analogies, or simply guesses. In many cases, significant uncertainty is associated with these data [23-29]. Therefore, optimization of a reaction mechanism is not only relevant for restoring the prediction ability of a reduced mechanism but also to improve the kinetics parameters within their range of uncertainty for reactions where the data are not established yet. In case the parameters are modified to values outside their known uncertainty limits, the physical meaning of the mechanism gets lost to some extent and the mechanism

degenerates into a complex data fit which may still be useful within the range of validity it was optimized for (that then must not be exceeded).

Many optimization techniques have been developed, some of them being gradient-based while others rely on heuristics and evolutionary algorithms.

Gradient-based optimization methods direct the search in the direction of the steepest gradient of the objective function to find its minimum [30, 31]. The gradient-based methods are often extended by applying sensitivity analysis to identify the principal components of the system [32, 33]. However, the gradient-based methods capture only the local optimum of the objective function which is inconvenient for systems with multiple optima that are typical for chemical kinetics problems. Frenklach et al. [34] proposed the solution-mapping method, a computationally efficient optimization method based on the objective function surface approximation by polynomial response surfaces. These surfaces are obtained from a number of numerical experiments and approximate the landscape of the objective function instead of its real values. The objective function usually has a highly complex structure with multiple local minima and maxima, which result from the small number of numerical experiments (that provide independent constraints on active parameters considered for the optimization) compared to the number of active parameters. The method yields a number of indistinguishable solutions, giving evidence for the lack of solution-uniqueness [34]. Relying on the solution-mapping method, Sheen and Wang [35] proposed quantification and minimization of the rate coefficients uncertainties based on polynomial chaos expansions (MUM-PCE), which was later used by Cai and Pitsch, [36] and Xin et al. [37] for the model calibration and the uncertainty estimation. Xin et al. [37] also investigated and presented correlation between the model uncertainty and the model completeness.

Genetic algorithms have shown to be particularly suitable for handling complex objective functions over a multidimensional search space. Polifke et al. [38] implemented genetic algorithms for optimizing a simplified two- and three-step methane-oxidation mechanism to match the heat release and net species production rates for premixed laminar flames. Harris et al. [39] used genetic algorithms to solve the inverse problem of determining the rate parameters that would match the measured species concentrations for hydrogen combustion. This approach was successful in retrieving rate coefficients that give accurate predictions for the investigated data set. Aiming to cover measurements different to those used in the optimization proposed by Harris et al. [39], Elliott et al. [40] extended the objective function of Harris' method to predict measurements of species concentration profiles for both laminar flames and perfectly-stirred reactors (PSR). Further on, to expand the validity range of the optimized mechanisms beyond the conditions used in the optimization, Elliott et al. [41] incorporated the predefined boundaries of the rate coefficients taken from the NIST (National Institute of Standards and Technology) chemical kinetics

database. Later, Elliot et al. [42] improved the multi-objective genetic algorithm to determine the Arrhenius coefficients and to recover observed species concentrations under different sets of operating conditions. Perini et al. [43] used a single objective, binary coded genetic algorithm for optimization of the pre-exponential factors and activation energies of selected reactions for ethanol oxidation. They adapted the objective function from [42] to account for the time evolution of the species. Allowed extent of change was fixed ±15% for the activation energy and ±80% for the pre-exponential factor, based on the average uncertainty range for ethanol combustion taken from NIST database. Aldawood et al. [44] used a multi-objective genetic algorithm to optimize a model for homogeneous-charge compression ignition (HCCI) against twelve sets of experimental data. The mechanism was treated together with the reactor model, i.e., three Arrhenius equation coefficients and four variables relevant for the simulated stochastic reactor model, were optimized at the same time.

This paper presents one possible optimization strategy based on a genetic algorithm, which is consistent to our reduction method [1]. Furthermore, the present study offers analysis of the objective function terms and the behavior of the algorithm and its solutions in context of the reaction rate optimization which have not been thoroughly tested, analyzed and discussed in sufficient detail before. The genetic algorithm was chosen for being reliable and robust, not requiring detailed knowledge about specific chemical processes from the user, and being generally applicable and well documented. To reduce the dimensionality of the search space, the forward rate constant is modified until the performance of the reduced mechanism is maximized in terms of the objective function. The modification of the rate constant corresponds to the modification of the pre-exponential factors in Arrhenius-type reactions. Modification of the forward rate constants applies to all types of reactions in the mechanism. Although the uncertainty of the kinetic data in a “detailed” mechanism is an important issue to consider, the present study is focused on the optimization itself. However, our approach offers an effective, easy-to-use way for maintaining the faithfulness to the established reaction coefficients in the original mechanism which is taken as a reference. For that purpose, we introduce a penalty function that constrains the modifications to avoid that the reaction-rate constants deviate too much from well-established values. The effectiveness of the penalty function approach is established by a comparison to the optimization with predefined uncertainty bounds, and it is shown that for an appropriately reduced mechanism, a reasonably stringent penalty function will keep the rate constants within their uncertainty ranges while restoring good accuracy over a given range of conditions (Appendix D). As the previously published reduction technique [1] is a small subset of the optimization technique presented here, a further reduction of the mechanisms can be achieved if the penalty function is set to favor reaction rate constants with a value of zero (sections 3.2 and 4.2).

2. Genetic algorithm-based optimization

Genetic algorithms mimic natural evolution for solving optimization problems [45] and are well suited for problems with multiple solutions in a large search space [46]. The original concept of the genetic algorithm was introduced by Holland in 1975 [47]. The core of each optimization algorithm is the objective function, which is essentially a communication tool between the algorithm and the search space. The requirements for the solution are defined by the objective function, which evaluates the performance of each candidate solution and assigns a fitness value to it. The optimal solution is then found with respect to the objective function. The candidate solution is encoded in a way to be efficiently handled by the genetic algorithm. For the particular problem of the mechanism optimization, the candidate solution is a mechanism encoded as a set of normalized reaction-rate constants, a so-called real-value chromosome with each individual coefficient being called a gene. The objective function handles the candidate solution in its real form, as a reaction mechanism used for example in a homogeneous-reactor simulation. The genetic algorithm itself operates on the problem's chromosome representation.

The genetic algorithm can be summarized as follows:

1) *Initialization* by generating the initial chromosome population
2) *Evaluation* of the performance of each chromosome (by comparing the results of the reduced and detailed mechanism in flame or reactor simulations)
3) *Selection* of the fittest chromosomes (parents) from the current population to yield the next generation of chromosomes
4) *Crossover* of the selected chromosomes in order to exchange genes to produce new chromosomes (children) for the next generation
5) *Mutation* by a small change to the children chromosomes which increases the diversity of the population and avoids falling into local minima

Steps 2 to 5 are repeated until pre-defined termination criteria are satisfied. The problem-specific genetic algorithm operations are described in the following sections.

2.1. Encoding

The starting point of the optimization technique is the reduced mechanism with N_r reactions. The aim is to alter its reaction-rate coefficients until the prediction quality of the mechanism, relative to the reference, has been improved. The chromosome that corresponds to this mechanism is a real-value

ordered set of corresponding reaction-rate coefficients which are scaled against their original values such that $k_{i,\mathrm{opt}} = \alpha_i \; k_{i,\mathrm{ref}}$, where $k_{i,\mathrm{opt}}$ and $k_{i,\mathrm{ref}}$ are the optimized and the original forward rate-constants of the i^{th} reaction, respectively. For reversible reactions, the reverse rate constants are calculated by the law of mass action. Each scaled rate constant α_i (i = 1, …, N_r) is chosen from $\mathbb{R}^+$, so that the chromosome forms a continuous search space of dimension N_r. The scaling of the rate constant corresponds to the scaling of the pre-exponential factor of an Arrhenius rate expression for the reactions following the Arrhenius law. Normalizing the rate constants leads to an initial population with all scaling factors set to a real value of 1.0. Using an unchanged mechanism in contrast to a random seed as a starting point of the optimization helps to avoid a purely random optimization search and ensures numerical stability of the first solutions. The rate constants are altered for the first time in the mutation step.

2.2. Selection, reproduction, and mutation operators

The objective-function value for a single chromosome determines whether this chromosome will be selected for the next generation. Our approach employs a tournament selection [48-50] which randomly takes two or more chromosomes from the population of N_{pop} chromosomes and chooses the one with the smallest objective-function value amongst them. This is repeated N_{pop} times. The fittest chromosomes are generally preferred but some less fit chromosomes can contribute diversity. The selected chromosomes pair up to exchange the information between each other and create new children chromosomes (solutions) that are often superior to their parents. In this study a uniform crossover was chosen: Each gene has a 50% chance to be swapped between the mother and the father chromosome (Figure 1). Although it is the most important part of the genetic algorithm, the crossover on its own is not sufficient for the algorithm to find the optimal solution, because it only exploits the existing gene values without introducing new values. The mutation introduces a small variation to a randomly chosen subset of genes from one chromosome to maintain additional diversity and prevent getting stuck in the local minima – by introducing new values that were not found in the existing solutions. It is the iterative combination of the crossover and the mutation which enables the genetic algorithm to find a global optimum. In our mutation approach, these gene alterations are random normally-distributed variables $G(\mu,\sigma)$ with a mean μ and a standard deviation σ. This additive Gaussian mutation alters a gene x to a new value $x + G(\mu,\sigma)$. For non-negative genes x (scaling factors α) that can vary several orders of magnitude, a multiplication with positive normally distributed random variables is more suitable, leading to a new gene $xG(\mu,\sigma)$ after mutation, as the multiplication gives a log-normal distribution of the random-walk final values. The multiplicative mutation was chosen for the present study. Both additive and multiplicative Gaussian mutations are suitable for gene values within a highly dimensional search space [51-53]; further

discussion is presented in Appendix B. Other types of genetic algorithm operations are available as well, but the adopted ones have been shown to provide good robustness and convergence speed within our application. It should be noted that the choice of the operators does not affect the results, but only the convergence speed of the method.

During the evolution, there is a risk of losing the best chromosomes due to the crossover and the mutation. This problem is avoided by copying the fittest chromosomes from the current generation to the next generation without any change, which is known as elitist selection.

3. Objective function

The objective function evaluates the performance of the mechanisms from the population. The search is directed towards the solution with the smallest possible value of the objective function. The general form of the overall objective function which covers C different physical conditions is given by Equation 1 in terms of the single objective functions f_{obj} corresponding to each condition c.

$$f = \frac{1}{C}\sum_{c=1}^{C} f_{\mathrm{obj},c} \tag{1}$$

The objective function f_{obj} for each single condition depends on the evaluation terms $f_{\xi,i}$ for each of the reacting case-specific properties and their weighting factors w_i (Eq. 2).

$$f_{\mathrm{obj}} = \sum_{i=1}^{I_c} w_i f_{\xi,i} \Big/ \sum_{i=1}^{I_c} w_i \tag{2}$$

The evaluation terms consider criteria ξ that are essential for the application of the reduced mechanism. Common examples for ξ are the ignition delay time τ_{ign}, the temperature T, the mole fraction of a species s X_s, or the laminar flame speed s_{L}. The choice of the optimization targets, especially the important species, depends on the later application of the optimized mechanism. There is hence no unique definition of which optimization targets are important.

These evaluation terms in Eq. 2 are scaled and weighted to account for different orders of magnitudes for different optimization targets (properties ξ) and make the optimization flexible and easily adjustable to the desired output. The scaled terms are combined into one overall objective function (Eq. 2) for multiple conditions (Eq. 1). There are many ways to scale or normalize the evaluation terms. Chosen are expressions that not only restrict the single error contributions to a comparable range but also allow variable weighting of the error itself. Various expressions were tested, and we selected those which enable

the easiest setting of the desired optimization objectives. The objective function has two aspects, first is the accuracy of the optimized mechanism and second is imposing constraints to the mechanism modifications; both are discussed below. It is important to emphasize that the normalization expressions and the coefficients are problem-dependent. Thus, an appropriate choice can be made empirically, based on preliminary optimization runs consisting of only few generations.

3.1 Accuracy criteria

Optimization targets involving accuracy are normalized according to their nominal values ξ_{ref}. The deviation between the reference (ξ_{ref}) and the optimized mechanism (ξ_{opt}) is normalized using the logarithmic expression (Eq. 3, Figure 2a) introduced before [1].

$$f_{\xi} = \ln\left(1+\sigma\left|\frac{\xi_{\text{opt}}-\xi_{\text{ref}}}{\xi_{\text{ref}}}\right|\right) \tag{3}$$

When $\left(\xi_{\text{opt}}-\xi_{\text{ref}}\right)$ is a set of discrete function values, the dimensionless deviation ξ_{profile} is calculated from the integral over the entire profile along *x* (Eq. 4).

$$\xi_{\text{profile}} = \frac{1}{A_{\text{ref}}}\int\left|\xi_{\text{opt}}(x)-\xi_{\text{ref}}(x)\right|dx \tag{4}$$

The bounding-box area A_{ref} is spanned orthogonally by the reference mechanism's values ξ_{ref} along the simulation range Δx (flame coordinate or time), according to Eq. 5.

$$A_{\text{ref}} = (\xi_{\text{ref,max}}-\xi_{\text{ref,min}})\Delta x \tag{5}$$

The area A_{ref} is independent of the profile's shape. The resulting, relatively small values of ξ_{profile} can be easily normalized (Eq. 6) and incorporated into the overall objective function.

$$f_{\xi} = \frac{2}{1+\exp\left(-\sigma\left|\xi_{\text{profile}}\right|\right)}-1 \tag{6}$$

This normalization restricts the error $\xi_{profile}$ to the interval [0, 1] and its steepness can be adjusted by the sharpening factor σ (Figure 2b). The sharpening factor dictates how strong the target ξ_{opt} is directed towards its optimal value ξ_{ref} (Figure 2). The value of σ is chosen based on the nature and the relevance of the optimization target ξ, therefore the choice of σ is always problem dependent. Small values of σ for some targets are sufficient to continuously direct the targets to their reference value, while for other targets, a very strong directing towards their desired value may be necessary. The appropriate choice of σ is always made empirically, based on the resulting values of ξ for a sample set of chromosomes, to make the optimization target weighting suitable for the overall objective function.

The normalization enables flexible adjustment of the evolution pressure for any part of the objective function thus enabling an optimal combination of accuracy targets to be found in a transparent way.

3.2 Penalty function

The modifications to the model during the optimization can be constrained by introducing penalty terms into the objective function. In this work, the constraint is imposed onto each gene (reaction rate constant) of the chromosome, by penalizing deviations of the rate constant from the wanted value given as a parameter to this function. The constraints are user-defined, depending of the optimization preferences, which may be minimal possible rate modifications, drawing certain rates towards zero or any other limiting value for certain reaction rates. We mainly use the penalty function to keep the reduced reaction coefficients near to their original values, but have also applied the penalty function for further reductions of the mechanisms. Both applications are discussed and tested below.

Faithfulness to the original reaction mechanism

The basic optimization of the (reduced) mechanism considers the rate coefficients of the original mechanism as an initial value, from which the optimization is started – so that the values can be changed by a very large degree. This approach would hence neglect the chemical and physical knowledge that is already involved in these reaction coefficients, albeit with some (often large) uncertainty. To keep the reduced mechanism faithful to the original reactions, we have introduced a component to the objective function that penalizes large deviations from the original values, an approach not dissimilar to previous work by Sheen and Wang [35], Cai and Pitsch [36] and Xin et al. [37]. Their optimization and calibration of the pre-exponential factors requires the individual uncertainty factors to be known. These uncertainty factors are used to divide the reactions into a well-known and poorly-known class. The normalization of the pre-exponential factors depends on this classification and includes the uncertainty factors. The penalty term [35–37] is then only applied if the pre-exponential factors are well measured and it is defined as a

sum of weighted squares of the normalized pre-exponential factors. The expression (Eq. 7) chosen in the present work has the advantage of enabling a more general and flexible way for constraining the model modifications even if the uncertainty factors of the elementary reactions are not known. The penalty function f_{pen}, which keeps the rate constant $\alpha_{i,\text{opt}}$ of the reaction i close to the given value $\alpha_{i,\text{ref}}$ by penalizing significant modifications of $\alpha_{i,\text{opt}}$ relative to $\alpha_{i,\text{ref}}$ is expressed as:

$$f_{\text{pen}} = \frac{1}{N_r}\sum_{i=1}^{N_r} f_{\text{pen},i}$$
$$f_{\text{pen},i} = \frac{2}{1+\exp\left(-\sigma\left|\alpha_{i,\text{opt}} - \alpha_{i,\text{ref}}\right|\right)} - 1 \qquad (7)$$

The value of $\alpha_{i,\text{ref}}$ determines the purpose of the penalty function: a value of $\alpha_{i,\text{ref}} = 1.0$ keeps the rate constants close to their nominal values, a value of $\alpha_{i,\text{ref}} = 0.0$ drives the optimization towards eliminating further reactions, as discussed below. Depending on the choice of the σ value, Eq. 7 may behave as a linear, logarithmic, sigmoidal or a step-function within a limited range of α values (Fig. 2b). The use of the penalty function which may consider specified constraints to the reaction rates is demonstrated in Section 4.1 of this paper. It should be noted that an ideal penalty function could be set for each reaction, with a weight scaled by the uncertainty of each specific reaction. The effort in obtaining a complete uncertainty vector can however be prohibitive, in particular, for more advanced and sizeable mechanisms, which is why we prefer applying the same penalty function to all reaction rates.

Elimination of reactions

The penalty function can also be used for the further reduction of the mechanism during the optimization by driving very small reactions coefficients k towards zero, so that the reaction can be removed. The reduction is forced by setting the value of $\alpha_{i,\text{ref}}$ in Eq. 7 to zero. From Fig. 2c it can be seen that the α values close to the reference value α_{ref} are strongly pushed towards it. In the plateau of the function, no constraints to the gene alterations are imposed.

4. Results

The optimization method was demonstrated for the GRI-Mech 3.0 methane combustion mechanism [54] and for a *tert*-butanol mechanism [55], which were previously reduced using a genetic algorithm-based method [1] and a homogeneous reactor model [56] for evaluation. It is important to emphasize that

the GRI-Mech 3.0 is already optimized and that the further optimization of the mechanism reduced from it might violate the physically determined uncertainty ranges of some reactions. As described in the introduction, this is acceptable in the context of this paper where reduced and optimized mechanisms will only be used within the range of conditions they have been designed for. For the mechanism reduced from GRI-Mech 3.0, we demonstrate the optimization under six operating conditions with a minimum deviation from the original reaction rates. For the *tert*-butanol combustion, we demonstrate the further reduction of the mechanism through suitable parameters of the penalty functions.

4.1. Optimization of a reduced methane mechanism

Prior to the optimization, the GRI-Mech 3.0 mechanism had been reduced to 52 reactions and 26 species by removing 273 reactions and 27 species for a homogeneous combustion at atmospheric pressure, stoichiometric methane/air mixture and an initial temperature of 1400 K [1]. The reduction criteria were the ignition delay time, final temperature, number of reactions, and the computational time required for the solution of a homogeneous reactor problem [1]. The computational time and the number of reactions were taken as the reduction criteria to avoid possible stiffness and numerical instabilities that may occur due to eliminating reactions. The result is a reduced mechanism that is small in size and fast in computation for an intended application. The reduction had successfully preserved the ignition delay times and the final temperature predictions, but the predictions of intermediate species concentrations were disturbed. The present paper shows significant improvements of the intermediate species predictions by optimizing the rate coefficients of the remaining reactions in the reduced mechanism under various operating conditions (cf. Table. 1). The objective function incorporates the ignition delay time, the temperature profile, the maximum value of OH mole fraction, the hydrogen-atom mole fraction profile and its maximum value (Table 2). Atomic hydrogen was chosen for its strong impact on laminar flame speed [57]. A penalty function was set up to constrain the change in rate coefficients. The optimization was performed using the same accuracy criteria for each condition. The overall objective-function value evolution for a population of 48 chromosomes is illustrated in Fig. 3, showing the convergence of the optimization where satisfactory results were achieved after approximately 100 generations (The best individual within 1000 generations appeared in generation 984). The mechanism's performance is shown in Figs. 4 and 5 for the reactor calculations under various operating conditions. For equivalence ratios ϕ of 1 and 0.67 under atmospheric (Fig. 4) and elevated pressure (Fig. 5), the profiles of temperature and OH, CO_2, and H_2O mole fractions were almost completely restored to the results from the full mechanism. For $\phi = 2$ these profiles were also improved, but not completely restored, implying that the reduction removed reactions that are important at high equivalence ratios.

Figure 6 shows the behavior of the objective function terms for the optimized mechanism for six operating conditions. Although the objective function is minimized for all the conditions, no significant improvement is obtained for the high equivalence ratio cases 3 and 6. A large mismatch between the optimized and the reference mechanism can be seen for OH profile for $\phi = 2$ (Fig. 4). However, the OH profile was not considered by the objective function but only its maximum value, which is significantly improved (Fig. 6). Due to the fact that the objective function is a linear combination of single objective function terms, the global minimum of the overall objective function will normally deviate from the global minima of its elements.

4.2. Further reduction and optimization of a *tert*-butanol mechanism

A *tert*-butanol combustion mechanism [55] with 2342 reactions and 431 species was first reduced to 248 reactions and 198 species using the method described by Sikalo et al. [1] and then optimized using the genetic algorithm-based technique presented in this work. The objective function for the reduction included the ignition delay time, final temperature, the number of reactions and the computational cost (CPU time). For the objective function, stoichiometric *tert*-butanol/air combustion was simulated for a constant pressure (atmospheric) homogeneous reactor with an initial temperature of 1200 K. Operating conditions of the reactor simulation were the same for both the reduction and the optimization. The optimization criteria were the ignition delay time, the temperature (maximal value and the temporal variation), and the mole fractions of the important radicals (H, OH, and CH_3). The reference was the original mechanism. Table 3 lists the considered properties and their normalization functions used in the objective function.

To test the newly introduced penalty function in respect to the optimization objective of the *tert*-butanol mechanism, ten optimization runs were performed. These runs have the same operating conditions and accuracy criteria, but the penalty functions (Eq. 7) have different parameters α_{ref}, w_i and σ (Table 4).

The highest degree of further reduction was achieved in run 7 where the penalty for the size of the mechanism had the highest weight ($w_i = 6.0$). In this case, the penalty function increased the evolution pressure towards further elimination of 27 reactions during the optimization. The optimization run took about 60 hours for 2000 generations on 48 AMD Opteron 2.6 GHz cores. The evolution of the overall objective function value for a population size of 96 is displayed in Fig. 7 (top) for the simulation run 7 (Table 4), showing a significant kink in convergence at generation 375 and overall slow convergence. The behavior of the accuracy criteria is illustrated in Fig. 7 (center) as evolution of the peak value of atomic

hydrogen, which converged already in generation 375. At this generation, the mechanism consisted of 246 reactions. From this generation on, only the highly-weighted penalty criterion was subject to the optimization, reducing the mechanism to 221 reactions in generation 1998 (Fig. 7, bottom) without further improvement to accuracy. The optimization was terminated after 2000 generations.

Figure 8 illustrates the performance of the full, the reduced, and the optimized *tert*-butanol mechanism for runs 1, 2, and 7 showing a significant improvement of the optimized mechanism over the un-modified reduced mechanism for any case. This demonstrates that both objectives, accuracy and further reduction, can be achieved at the same time.

4.3. Parameter study of the penalty terms

To obtain a better understanding of the influence of the penalty terms on the evolution and the results, we compared the values of the single objective-function terms for the reduced and optimized mechanisms from runs 1–10 in Figure 9. Figure 10 illustrates the discrete probability density of the rate values of the optimized mechanisms in runs 1–10 influenced by the penalty functions. The runs in Table 4 are ordered in the first place according their penalty terms: the run without penalty (run 1), the runs with penalties aiming to preserve the nominal α values (runs 2 and 3), the runs aiming to eliminate reactions (runs 4–7) and the runs combining the conflicting penalty terms (runs 8–10). Weights of the penalty terms vary from small to large values, as well as the corresponding sharpness. The parameters in Table 4 are chosen in a way that enables the comparison between the different runs. Only one run is performed per optimization setup to indicate the influence that the weights and the sharpness values have on the penalty terms. Various and even conflicting penalty terms (runs 8, 9, and 10) were set to test their influence on the accuracy, and to gain a better understanding about how the penalty function affects the modification of the reaction constants. As the mechanism was reduced and optimized under the same conditions, all runs show significant improvement in terms of accuracy (Fig. 9 and partially Fig. 8), indicating that the optimization can still enhance the mechanism's performance even with the constraints imposed on the model modifications. The standard deviation and the mean of the normalized rate coefficients for all runs are shown in Table 5. It can be seen from Tables 4 and 5 that the standard deviation can be adjusted straight forward via the weights of the penalty terms.

To illustrate the influence of the penalty term parameters on the objective function evolution, the overall objective function, the objective-function term $f_{H,max}$ and the penalty terms for runs 2 and 8 are shown in Figs. 11–13. The aim of the penalty term for run 2 was to maintain the faithfulness to the original reaction rates with a small sharpness value in Eq. 7 ($\sigma = 4$). The penalty term of run 2 starts from

0.0 and converges relatively fast, which helps the overall objective function to converge along with the accuracy.

The evolution of the objective function terms for the case where the penalty term features two conflicting goals, aiming to either remove unnecessary reactions by driving the rate coefficients to zero and to maintain the original value of rate coefficients at the same time (cf. Table 4), is illustrated for run 8 in Figs. 12 and 13.

The behavior of the penalty term which prefers values of 1.0 (Fig. 13, bottom) is similar to that from run 2 (Fig. 11, bottom). The penalty term that prefers values of 0.0 is comparable to that from run 7, albeit with significantly lower weight. Therefore, the penalty term from run 2 does not significantly contribute to the overall convergence of the objective function (Fig. 12).

The standard deviation of the resulting normalized rate constants for all runs with $\alpha_{ref} = 0.0$ increases when the weight for the corresponding penalty term increases and their probability density (Fig. 10) is flattened. For the runs 2, 8, and 9, the standard deviation decreases as the weights of the penalty terms decrease and their probability density is narrower. The value of α is not biased in run 1; however its standard deviation and the mean are close to 1. The plateau region of the penalty function (Fig. 2c) in runs 6, 7, and 10 is responsible for a not-constrained change of larger α values, while very small α values are steeply directed towards α_{ref}. The tendency towards further reduction cannot be recognized from the means of runs 6 and 7 (both means are close to 1) but the reduction trend is more visible from their corresponding discrete probability densities (Fig. 10). It can be also seen in Fig. 10 that high weights in runs 6 and 7 force the values of α towards zero. Although the penalty weight for run 6 is smaller than the weight for run 7, the mean for run 7 is greater than the mean of run 6, indicating that the bias towards $\alpha = 0$ is not crucial for the distribution of α. For runs with higher weights towards 0.0 (runs 6, 7, 10, and, less obviously, 5) in Fig 10 we see that the bias towards 0.0 is somewhat compensated by an increased standard deviation. From that, we conclude that the reduction requires significant modification of the original system if the accuracy is to be retained. The mean and the standard deviation for the runs with opposed penalty terms (8, 9, and 10) are consistent with those for runs with single penalty terms, and while their accuracy is retained, the reduction effect is not significant. Runs with small weights of the penalty terms which direct α values towards 0.0 (runs 4 and 5) were not able to reduce the mechanism further.

The predefined uncertainty bounds for each elementary reaction in the mechanism can however be considered within the optimization procedure if required. The behavior of such an approach is investigated as well and demonstrated in Appendix D for mechanism [58], with well-documented uncertainty factors for each elementary reaction. The optimization with the penalty function is compared

against the optimization with predefined uncertainty bounds and the results indicate that, for a well posed mechanism, the presented penalty function is not only easy to use and keeps the rate coefficients within their uncertainty ranges, but that it also keeps most coefficients faithful to their original value: with the penalty function, only few coefficients deviate from their original value, so that only these must be documented, communicated and adjusted. As the few resulting changes can be clearly attributed to few reactions, it is possible to understand and analyze the effect of these modifications. We consider this a clear advantage of the penalty function over just enforcing the uncertainty limits, which is shown in Appendix D to cause a wide scatter of all rate coefficients over full range of uncertainty.

Conclusions

A genetic algorithm-based methodology for optimizing reduced reaction kinetics mechanisms has been developed. The method is designed to enhance the prediction quality of (reduced) reaction mechanisms under multiple operating conditions using zero and one-dimensional simulations, for example in a homogeneous reactor or a laminar flame. The mechanisms can be optimized against the original detailed mechanism, another detailed mechanism, or available experimental data. The optimization is performed by tuning the reaction rate constants of the target mechanism's reactions until the convergence criteria in terms of the objective function are satisfied. The objective function is designed to enable flexible adjustment of the criteria and to direct the optimization towards the user's requirements for a desired application of the mechanism. Besides the accuracy criteria, a penalty function is introduced to either minimize the extent of change introduced to the original rate-constants, or even to reduce the mechanisms further. Both objectives are shown to work properly. The same penalty function is applied to all reactions in the mechanism. By keeping all the reaction rate constants close to their nominal values, we avoid the additional complexity, save the effort for searching hundreds or thousands of uncertainties for the specific rate constants from the databases, and do not need to guess the uncertainties that are not well established. Specifically, the penalty approach is more flexible, easy to parametrize, the extent of rate modifications is overall lowered, the resulting rates are less scattered and the few altered reactions are easy to document, communicate and analyze. The performance of the optimization was demonstrated for strongly reduced methane mechanism (derived from GRI-Mech 3.0) and a reduced *tert*-butanol combustion mechanism, for which a fair compromise of accuracy, size reduction and near-original reaction coefficients has been achieved.

Acknowledgements

The authors would like to thank to Dr. Mustapha Fikri (IVG-RF, University of Duisburg-Essen) for helpful discussions.

References

[1] N. Sikalo, O. Hasemann, C. Schulz, A. Kempf, I. Wlokas, Int. J. Chem. Kinet. 46 (2013) 41-59.
[2] A. S. Tomlin, T. Turányi, M. J. Pilling, Compr. Chem. Kinet. 35 (1997) 293-437.
[3] T. Lu, C. K. Law, Prog. Energ. Combust. 35 (2009) 192-215.
[4] A. S. Tomlin, M. J. Pilling, T. Turányi, J. H. Merkin, J. Brindley, Combust. Flame 91 (1992) 107-130.
[5] H. Wang, M. Frenklach, Combust. Flame 87 (1991) 365-370.
[6] T. Turányi, New. J. Chem. 14 (1990) 795-803.
[7] M. Valorani, F. Creta, D. A. Goussis, J. C. Lee, H. N. Najm, Combust. Flame 146 (2006) 29-51.
[8] T. Lu, C. K. Law, Proc. Combust. Inst. 30 (2005) 1333-1341.
[9] T. Lu, C. K. Law, Combust. Flame 146 (2006) 472-483.
[10] J. Revel, J. C. Boettner, M. Cathonnet, and J. S. Bachman, J. Chim. Phys. Phys. Chim. Biol., 91 (1994) 365-382.
[11] I. P. Androulakis, J. M. Grenda, J. W. Bozzelli, AIChE Journal 50 (2004) 2956-2970.
[12] K. He, I. P. Androulakis, M. G. Ierapetritou, Chem. Eng. Sci. 65 (2010) 1173-1184.
[13] J. Wei, J. C. W. Kuo, Ind. Eng. Chem. Fundam. 8 (1969) 114-123.
[14] H. Rabitz, G. Y. Li, J. Toth, Chem. Eng. Sci. 49 (1994) 343-361.
[15] A. S. Tomlin, G. Y. Li, H. Rabitz, J. Toth, SIAM J. Appl. Math. 57 (1997) 1531–1556.
[16] E. Ranzi, M. Dente, A. Goldaniga, G. Bozzano, T. Faravelli, Prog. Energ. Combust. 27 (2001) 99-139.
[17] A. Stagni, A. Cuoci, A. Frassoldati, T. Faravelli, E. Ranzi, Ind. Eng. Chem. Res. 53 (2014) 9004–9016.
[18] M. Bodenstein, Z. Phys. Chem, 85 (1913) 329-397.
[19] Ch. J. Montgomery, C. Yang, A. R. Parkinson, J. Y. Chen, Combust. Flame 144 (2006) 37–52.
[20] U. Maas, S. Pope, Combust. Flame 88 (1992) 239-264.
[21] H. Bongers, J. A. Van Oijen, L. P. H. De Goey, Proc. Combust. Inst. 29 (2002) 1371-1378.
[22] X. Gou, W. Sun, Z. Chen, Y. Ju, Combust. Flame 157 (2010) 1111-1121.
[23] K. Héberger, S. Kemény, T. Vidóczy, Int. J. Chem. Kinet. 19 (1987) 171-181.
[24] T. Nagy, T. Turányi, Procedia Soc. Behav. Sci. 2 (2010) 7757-7758.
[25] T. Nagy, T. Turányi, Int. J. Chem. Kinet. 43 (2011) 359-378.
[26] L. Varga, B. Szabó, I. Gy. Zsély, A. Zempléni, T. Turányi, J. Math. Chem. 49 (2011) 1798-1809.
[27] T. Nagy, T. Turányi, Reliab. Eng. Sys. Safe. 107 (2012) 29-34.
[28] I. Sedyó, T. Nagy, I. Zsély, T. Turányi, European Combustion Meeting, Cardiff, UK, 2011, Paper 163.
[29] T. Turányi, T. Nagy, I. Gy. Zsély, M. Cserháti, T. Varga, B. T. Szabó, I. Sedyó, P. T. Kiss, A. Zempléni, H. J. Curran, Int. J. Chem. Kinet. 44 (2012) 284-302.
[30] H. G. Bock, In: K.H. Ezbert, P. Deuflhard, W. Jäger, editors. Modelling of chemical reaction systems. Berlin: Springer; 1981.
[31] G. S. G. Beveridge, R. S. Schechter, Optimisation: theory and practice. New York: McGraw-Hill; 1970.
[32] H. Rabitz, M. Kramer, D. Dacol, Annu. Rev. Phys. Chem. 34 (1983) 419-461.
[33] H. Rabitz, Computers Chem. 5 (1981) 167-180.
[34] M. Frenklach, H. Wang, J. Rabinowitz, Prog. Energy Combust. Sci. 18 (1992) 47-73.
[35] D. A. Sheen, H. Wang, Combust. Flame 158 (2011) 2358-2374.
[36] L. Cai, H. Pitsch, Combust. Flame 161 (2014) 405-415.
[37] Y. Xin, D. A. Sheen, H. Wang, C. K. Law, Combust. Flame 161 (2014) 3031-3039.
[38] W. Polifke, W. Geng, K. Döbbeling, Combust. Flame 113 (1998) 119-135.
[39] S. D. Harris, L. Elliott, D. B. Ingham, M. Pourkashanian, C. W. Wilson, Comput. Method. Appl. M. 190 (2000) 1065-1083.

[40] L. Elliott, D. B. Ingham, A. G. Kyne, N. S. Mera, M. Pourkashanian, C. W. Wilson, Genetic and Evolutionary Computation Conference, Late Breaking Papers, GECCO, New York, 2002, 138-144.
[41] L. Elliott, D. B. Ingham, A. G. Kyne, N. S. Mera, M. Pourkashanian, C. W. Wilson, Ind. Eng. Chem. Res. 42 (2003) 1215-1224.
[42] L. Elliott, D. B. Ingham, A. G. Kyne, N. S. Mera, M. Pourkashanian, C. W. Wilson, Progr. Energy Combust. Sci. 30 (2004) 297-328.
[43] F. Perini, J.L. Brakora, G. Cantore, R.D. Reitz, Comb Flame 159 (2012) 103-119.
[44] A. Aldawood, S. Mosbach, M. Kraft, A. Amer, SAE Technical Paper Series, 2011-01-1783
[45] D. E. Goldberg. Genetic Algorithms in Search, Optimization and Machine Learning. Addison-Wesley, Reading, MA (1989).
[46] B. L. Miller, D. E. Goldberg, Complex Syst. 9 (1995) 193-212.
[47] J. Holland, Adaptation in Natural and Artificial Systems, Ann Arbor, MI: The University of Michigan Press, 1975.
[48] D. E. Goldberg, K. Deb, in: G. J. E. Rawlins (Ed.), Foundations of Genetic Algorithms, Morgan Kaufmann, Los Altos, 1991, 69-93.
[49] T. Blickle, L. Thiele, TIK-Report, Zurich (1995)
[50] J. Zhong, X. Hu, M. Gu, J. Zhang, Web Technologies and Internet Commerce (2005) 1115-1121.
[51] T. Bäck, H. P. Schwefel, Evolutionary Computation 1 (1993) 1-23.
[52] D. B. Fogel, J. W. Atmar, Biol. Cybern. 63 (1990) 111-114.
[53] R. Hinterding, Proc. of the International Conference on Evolutionary Computation, IEEE Press 1995, 384-389.
[54] G. P. Smith, D. M. Golden, M. Frenklach, N. W. Moriarty, B. Eiteneer, M. Goldenberg, T. C. Bowman, R. K. Hanson, S. Song, W. C. Jr. Gardiner, V. V. Lissianski, Z. Qin, http://www.me.berkeley.edu/gri_mech/ (accessed 01.10.2013)
[55] S. M. Sarathy, S. Vranckx, K. Yasunaga, M. Mehl, P. Oßwald, W. K. Metcalfe, C. K. Westbrook, W. J. Pitz, K. Kohse-Höinghaus, R. X. Fernandes, H. J. Curran, Combust. Flame 159 (2012) 2028-2055.
[56] D. Goodwin, "Cantera: An object-oriented software toolkit for chemical kinetics, thermodynamics, and transport processes", Caltech, Pasadena, 2009. [Online]. Available: http://code.google.com/p/cantera (accessed 01.10.2013)
[57] H. Bongers, L. P. H. De Goey, Combust. Sci. Technol. 175 (2003) 1915-1928.
[58] A. A. Konnov, Combust. Flame 152 (2008) 507-528.
[59] F. Westley. Table of recommended rate constants for chemical reactions occurring in combustion. No. NSRDS-NBS-67. National Standard Reference Data System, 1980.
[60] R. J. Kee, M. E. Coltrin, P. Glarborg, Chemically Reacting Flow: Theory and Practice, John Wiley & Sons, Inc., Hoboken, NJ, USA, 2003.

Appendix A: Laminar flame speeds

The reduction and optimization of the reaction mechanisms have been carried out for homogeneous reactor simulations only. This may raise the question of how well such mechanisms can work for phenomena that are affected by diffusive transport. While this is beyond the scope of the present paper, we also show laminar flame speeds that result from these reduced and optimized mechanisms for completeness.

The reduced and then optimized methane combustion mechanisms (based on GRI 3.0) were tested for a freely propagating laminar flame at two pressures (1 MPa, 0.1 MPa) and five equivalence ratios (0.5, 0.67, 1, 1.5, 2). The resulting laminar flame speeds are shown in Figure A1. The results show that for the present cases, the mechanism reduction introduces an error of approximately 10% which is reduced to 5% for the optimized mechanisms. A further error reduction is expected when including the laminar flame speed in the objective function for reduction and optimization – which is beyond the scope of the present paper.

Appendix B: Influence of mutation on the modification of reaction constants

The mutation type used in the present study was multiplicative Gaussian mutation described in section 2.2. However, for the sake of completeness, we demonstrate the influence of both the additive and the multiplicative Gaussian mutations on the resulting normalized rate constants.

The modification of the rate constant scaling factors α away from the values in the previous generation is achieved by mutation, and the only place where the values of α themselves influence the objective function is in the penalty function. The influence of the additive and the multiplicative Gaussian mutation types on the distribution of the resulting normalized rate constants was tested using a full mechanism [55] in order to have a large number of samples (2342 genes). No accuracy criteria were considered in these runs. All the runs have the population size of 48 chromosomes and evolve within 1000 generations, using the uniform crossover and the tournament selection. Table B1 lists the initialization, the mutation types and the objective functions along with the standard deviations and the means of the resulting chromosome from these runs. Runs MR 1 and 2 have a constant objective function so that the final result is only influenced by the mutation and the crossover. The objective function for the remaining runs consists of the penalty function only.

The initial population for the runs MR 1–6 (Table B1) consists of the nominal values $\alpha = 1.0$, and the mutation introduces the first modification to the population. Since the minimum of the penalty function for runs MR 5 and 6 is already achieved in the initial population, the algorithm returns the nominal values

of α (Fig. B1). To see the influence of the mutation for a given $\alpha_{ref} = 1.0$ in the penalty function, the initial population consists of randomly chosen α values in the runs MR 7 and 8. The influence of the penalty function in MR 7 and 8 is visible in Fig. B1 (although the given number of generations was not sufficient to yield the resulting chromosome equal to that from MR 5 and 6, which is expected within the number of generations used for this comparison). The expected normal and the log-normal distributions of α values depending on the mutation type can be recognized from the discrete probability densities for all the runs (Fig. B1), even for the relatively small number of samples. For the optimization runs involving the accuracy criteria, the bias towards lower values of the rate constants is not dominant as it is for the runs involving the penalty function only. The influence of the mutation on the results is visible in runs from Table B1, because they do not involve the accuracy criteria. As previously stated in section 2.2, the mutation does not influence the optimization results but only the convergence speed in case the optimization is performed with the accuracy criteria.

Appendix C: Logarithmic scaling of rate constants in the penalty function

As an alternative to the penalty function used in the present study (Eq. 7) which is in an additive sense symmetric with respect to the given $\alpha_{ref} = 1.0$ value (Fig. 2c), one can impose the multiplicative treatment of the rate constants. The additive symmetric treatment means that, by using the penalty from Eq. 7 with $\alpha_{ref} = 1.0$, a rate scaling factor of 0.5 is equally treated as the scaling factor of 1.5 (i.e. they have the same penalty). If preferred, the multiplicative treatment of the scaling factors can be achieved by logarithmic scaling of the normalized rate constants within the penalty function:

$$f_{\mathrm{pen,log}} = \frac{2}{1+\exp\left(-\sigma\left|\ln\left(\frac{\alpha_{\mathrm{opt}}}{\alpha_{\mathrm{ref}}}\right)\right|\right)} - 1 \qquad (8)$$

This normalization is compared to the one that is used in the present study (Eq. 7) for various sharpness values (Fig. C1). The logarithmic normalization of scaling factor α cannot be applied for $\alpha_{ref} = 0$, which limits the use of Eq. 8 to $\alpha > 0$. For keeping the rate constants close to their nominal values ($\alpha_{ref} = 1.0$) with small σ, the function in Eq. 8 can be preferred over Eq. 7 if, for example, scaling factors of 0.5 and 2.0 are to be treated equally. However, for higher values of σ (as used in the present study), the difference between the functions defined by Eq. 7 and 8 becomes negligible (Fig. C1, $\sigma > 4$), implying that, for the algorithm, there is no effective difference between the two functions. This is consistent with the probability densities of the resulting α values from optimization runs 2 and 3 (Table 4, Figure 10). Here

Eq. 7, with σ of 4 and 20, is applied to the penalty function for $\alpha_{ref} = 1.0$, respectively. The mean values for the resulting normalized rate constants from runs 2 and 3 are both close to 1.0 (Table 5). We can therefore conclude that the formulation of Eq. 7 does not inherently bias the rate constants towards values lower than α_{ref} with the sharpness factors used for the present study. The logarithmic penalty function is applied to runs in Appendix D for completeness.

Appendix D: Consideration of predefined uncertainty boundaries of the reaction rates

Instead of using a penalty function, one could alternatively limit all rate constants to the uncertainty range of the reactions (provided that the uncertainties are known with low uncertainty). The behavior of such a strategy is investigated in the following section. For this study, the hydrogen combustion mechanism by Konnov (2008, [58]) with 33 reactions was selected for the following reasons: a) this mechanism is validated against a wide range of operating conditions, b) it was published with well-defined uncertainty factors UF for each elementary reaction, c) the hydrogen mechanism is small so that the resulting behavior can be analyzed and described in detail, and d) its reactions are an integral part of any hydrocarbon combustion mechanism.

The optimization method was altered such that the modified rate constants cannot exceed their uncertainty bounds $k/\mathrm{UF} < k < k\ \mathrm{UF}$ [58, 59]. The resulting optimized mechanism was then compared against the proposed penalty function approach described in section 3.2.

The hydrogen combustion mechanism was first reduced to introduce a perturbation to its prediction ability. The reduction was performed for a stoichiometric H_2/O_2 mixture diluted in Ar in a homogeneous reactor model under an initial temperature of 1200 K and a constant pressure of 0.2 MPa. For this study, two reduced mechanisms were selected, one "strongly perturbed (S)" with 11 reactions and one "weakly perturbed (W)" with 12 reactions. In the following, several optimization runs are presented to compare the effects of a) limiting the rate constants to their uncertainty range, b) the penalty function approach, and c) a combination of a) and b) on the resulting reaction rates and accuracy. Specifically, the optimization runs of the two reduced mechanisms aimed at restoring their accuracy with the following constraints to the rate modifications: a) none, b) with predefined UF, c) with the penalty function f_{pen} (Eq. 7) only, d) with a logarithmic penalty function $f_{pen,log}$ (Eq. 8) only, and e) with the combined constraints (uncertainty range defined with 2UF and f_{pen} and 2UF and $f_{pen,log}$). The accuracy criteria for all optimization runs were the same and involved the ignition delay time, temperature history and mole fraction history of H_2O_2 as an additional target for an intermediate species (Table D1).

The resulting reaction rate modifications from all optimization runs for both mechanisms are presented in Fig. D1, together with the uncertainty ranges for each reaction taken from the original publication [58]. Uncertainty limits were considered in four optimization runs, all of them with the same numerical setup and the same optimization criteria. The resulting reaction rate modifications for the UF-constrained cases and for one unconstrained run are presented in Fig. D1 (top). The resulting reaction rates from UF-constrained runs are quite scattered within their given uncertainty bounds, although they follow the same trend of modifications. The unconstrained run has a similar behavior as UF-constrained runs in terms of rate modifications for both mechanisms, except for one reaction rate that exceeds the uncertainty bounds (S2 for the strongly perturbed and W4 for the weakly perturbed mechanism, see Fig. D1).

The optimization results in terms of accuracy from these runs are shown in Figs. D2 and D3 for both mechanisms. Despite the different reaction rates for UF-constrained runs, the extent of accuracy restoration is identical for their corresponding mechanisms (Fig. D2 center, Fig. D7 and Fig. D3 center, Fig. D8). However, the extent of accuracy restoration was not the same for both reduced mechanisms using the constrained optimization. The constrained optimization did not fully restore the accuracy of the strongly perturbed mechanism (Fig. D2 center, Fig. D7), indicating that this mechanism was already distorted to an extent where some of the reactions (e.g., S2) must be modified beyond their uncertainty limits to fully restore the accuracy against the detailed mechanism. On the other hand, the unconstrained run (Fig. D2 left) fully restored the accuracy for this mechanism at the cost of exceeding the uncertainty of reaction S2. The accuracy of the weakly perturbed mechanism was fully restored for the UF-constrained and the unconstrained runs without exceeding the predefined uncertainty bounds (Fig. D3 left, Fig. D8).

The resulting reaction rate modifications for the optimization runs including penalty functions is presented in Fig. D1 (bottom) for both mechanisms. In comparison to the previous runs (Fig. D1, top), the reaction rates mostly remain close to their nominal values with exception of few reactions recognized as those that tend to exceed their uncertainties as seen in Fig D1 (top). Specifically, one reaction (S2) deviates from its nominal value and uncertainty bounds for the strongly perturbed mechanism, while all the other reactions remained close to their original coefficients – or within their uncertainties (although these were not considered in runs with penalty functions). For the weakly perturbed mechanism, the behavior of the rate modifications for runs including penalty functions is similar to the previous case, with somewhat bigger deviation of the rate constants for reactions W1 and W12 which, however, do not exceed their uncertainty bounds. The penalty function managed to restore the accuracy for both mechanisms as seen in Figs. D2–D5.

Combined constraints were imposed to test the effect of the penalty functions on the reaction rates in case when the uncertainty range is predefined but doubled (2UF). The idea behind this strategy was to evaluate if the penalty function would still bring the coefficients back into their original uncertainty bounds (UF) and restore the accuracy. The results of these tests in terms of accuracy are shown in Figs. D4 and D5 for two considered mechanisms. The accuracy of the mechanism that was strongly perturbed during the reduction was not fully restored for runs with combined constraints (Fig. D4 center and right), as the penalty functions strongly pushed all the reaction rates towards their nominal values and the reaction S2 towards its uncertainty bounds. However, the combined constraints gave better accuracy than simple UF-constraints for this mechanism (Fig. D4). For the weakly disturbed mechanism, all the runs successfully restored the accuracy and the reaction rates remained within their prescribed uncertainty bounds. This implies that, for strongly or inappropriately reduced mechanisms, the accuracy can be largely restored for a chosen parameter range at the cost of violating the physical reaction rate uncertainties. For well-posed or appropriately reduced mechanisms, the penalty function is able to keep the reactions close to their original values or within their uncertainty ranges, while still obtaining a plausible accuracy for a given range of optimization parameters.

To get a better insight into the behavior of the reactions that exceed their uncertainty limits, a sensitivity analysis for temperature and H_2O_2 in respect to the remaining reactions of two reduced mechanisms was performed; the results are shown in Fig. D6. Sensitivity coefficients were calculated as $\frac{A_i}{T}\frac{\partial T}{\partial A_i}$ for the temperature, and $\frac{A_i}{Y_{H_2O_2}}\frac{\partial Y_{H_2O_2}}{\partial A_i}$ for H_2O_2, respectively [56, 60]. Figure D1 shows that the most sensitive reactions (Fig. D6) remain unchanged (e.g., S7 (W7): H + O_2 ↔ OH + O) for both reduced mechanisms through all the optimization runs. The reactions that tend to fall outside their uncertainty bounds (S2 for the strongly perturbed, W1 and W12 for the weakly perturbed mechanism) show small sensitivity relative to other reactions.

In addition to Figs. D2–D5, the accuracy of the remaining optimization runs with predefined uncertainty factors UF repeated for the same conditions and criteria are shown in Figs. D7 and D8. The extent of modifications of the reaction rates for these runs is reported in Fig. D1 top (strongly perturbed and weakly perturbed reduced mechanism, respectively). Different reaction rate modifications resulted from each successive UF-constrained run for the corresponding mechanism (Fig. D1 top) but their prediction abilities were the same for the chosen optimization targets.

Tables

Table 1 Operating conditions for which the reduced GRI-Mech 3.0 mechanism was optimized.

c	ϕ	T_i / K	p / MPa
1	1	1400	0.1
2	0.67	1400	0.1
3	2	1400	0.1
4	1	1400	1
5	0.67	1400	1
6	2	1400	1

Table 2 Objective function parameters for optimization of reduced GRI-Mech 3.0.

ξ_i	w_i	Normalization	σ
τ_{ign}	1.0	Eq. 3	4
$T_{profile}$	1.0	Eq. 6	25
$X_{H,\,max}$	1.0	Eq. 3	4
$X_{OH,\,max}$	1.0	Eq. 3	4
$X_{H,\,profile}$	1.0	Eq. 6	25
$t(T_{max})$	1.0	Eq. 3	4
$\alpha_{i,ref} = 1.0$	1.0	Eq. 7	5

Table 3 Objective function parameters for the optimization of *tert*-butanol mechanism

Property	w_i	Normalization	σ
τ_i	1.0	Eq. 3	4
$t(T_{max})$	1.0	Eq. 3	4
T_{max}	1.0	Eq. 3	4
$T_{profile}$	1.0	Eq. 6	25
$X_{H,\ max}$	1.0	Eq. 3	4
$X_{OH,\ profile}$	1.0	Eq. 6	25
$X_{CH3,\ profile}$	1.0	Eq. 6	25

Table 4 Parameters of the penalty function for ten *tert*-butanol optimization runs. Preferred values of the rate constant is $\alpha_{i,\mathrm{ref}}$, weighting of penalty terms is w_i and σ is the sharpness of the penalty term normalization (Eq. 7).

Run	$\alpha_{i,\mathrm{ref}}$	w_i	σ
1	-	-	-
2	1.0	1.0	4
3	1.0	1.0	20
4	0.0	1.0	20
5	0.0	1.0	50
6	0.0	4.0	25
7	0.0	6.0	25
8	0.0; 1.0	0.5; 0.5	20; 4
9	0.0; 1.0	0.5; 0.5	20; 20
10	0.0; 1.0	6.0; 1.0	20; 4

Table 5 Overview of standard deviation, mean and the number of remaining reactions for ten optimization runs for the reaction of *tert*-butanol.

Run	Standard deviation	mean	N_r
1	1.092	1.063	248
2	0.817	1.022	248
3	0.897	1.095	248
4	1.278	1.049	248
5	1.323	1.065	247
6	1.548	0.813	226
7	1.836	0.977	221
8	0.757	1.01	248
9	0.728	1.018	248
10	1.324	0.693	227

Table B1 Overview of standard deviation and mean for eight mutation-test runs for the *tert*-butanol full mechanism.

Run	Mutation type	Objective function	Initial population	Standard deviation	mean
MR 1	multiplicative	const.	nominal	1.399	0.830
MR 2	additive	const.	nominal	2.405	2.997
MR 3	multiplicative	$f_{pen}(\alpha_{ref} = 0.0)$	nominal	1.356	0.611
MR 4	additive	$f_{pen}(\alpha_{ref} = 0.0)$	nominal	1.688	1.304
MR 5	multiplicative	$f_{pen}(\alpha_{ref} = 1.0)$	nominal	0.0	1.0
MR 6	additive	$f_{pen}(\alpha_{ref} = 1.0)$	nominal	0.0	1.0
MR 7	multiplicative	$f_{pen}(\alpha_{ref} = 1.0)$	random	2.478	2.806
MR 8	additive	$f_{pen}(\alpha_{ref} = 1.0)$	random	2.547	3.792

Table D1 Objective function parameters for optimization of reduced hydrogen mechanisms, including the penalty functions parameters for the runs where these were applied. The small values of the weighting factors w_i for the penalty terms are adjusted to the comparably small number of the remaining reactions.

ξ_i	w_i	Normalization	σ
τ_{ign}	1.0	Eq. 3	6
$T_{profile}$	1.0	Eq. 6	10
$X_{H2O2,\ profile}$	1.0	Eq. 6	10
$f_{pen}(\alpha_{ref} = 1.0)$	0.05	Eq. 7	4
$f_{pen,log}(\alpha_{ref} = 1.0)$	0.05	Eq. 8	4

Figures

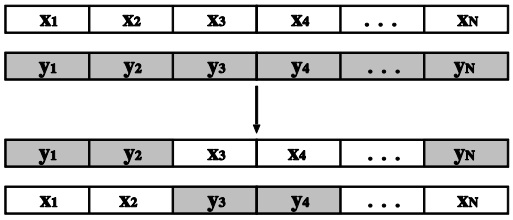

Figure 1 A uniform crossover between two parents

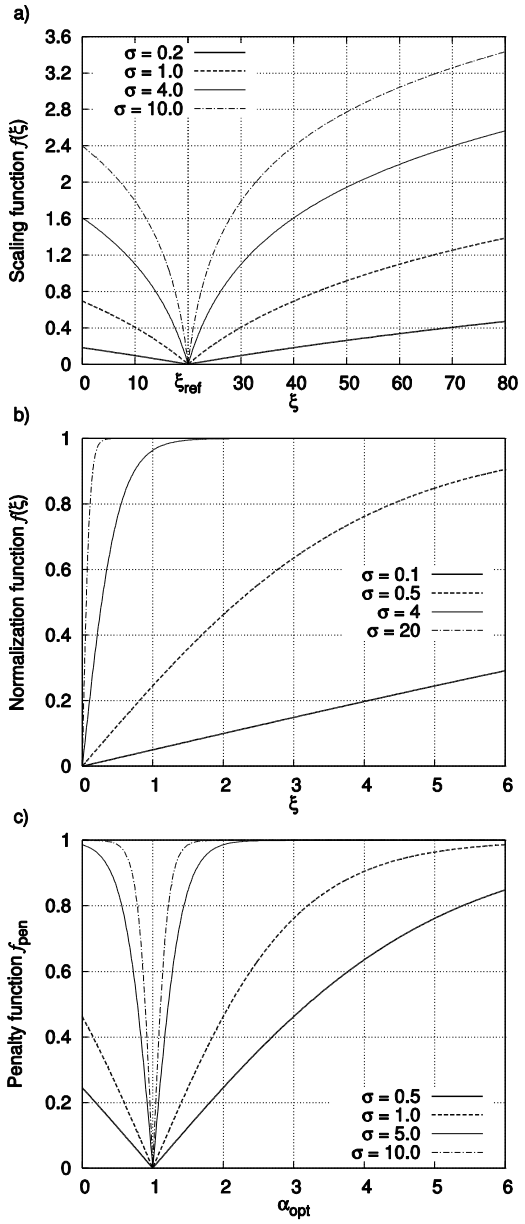

Figure 2 Logarithmic scaling of property ξ (a), sigmoid normalization (b) of a property ξ, and the penalty function $f_{\text{pen},i}$ where $\alpha_{i,\text{ref}} = 1.0$ (c). The penalty function for $\alpha_{i,\text{ref}} = 0.0$ is identical to that shown in (b).

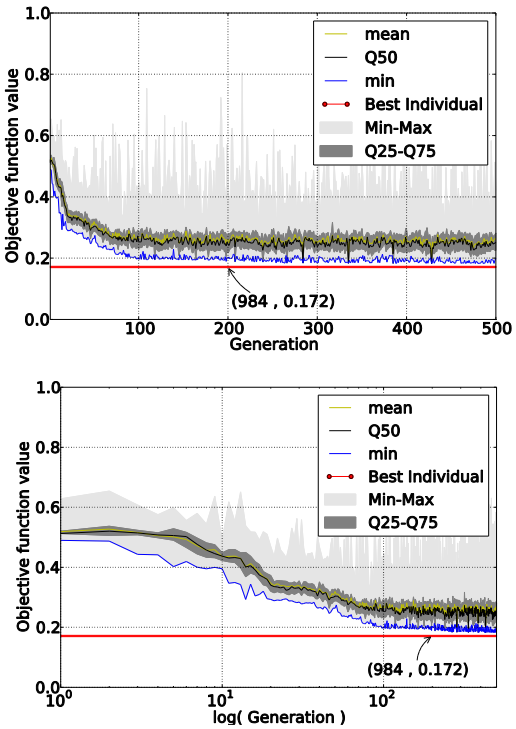

Figure 3 Evolution of the objective function value for the methane/air mechanism optimization. Red line denotes the objective function value of the best individual which was found over 1000 generations.

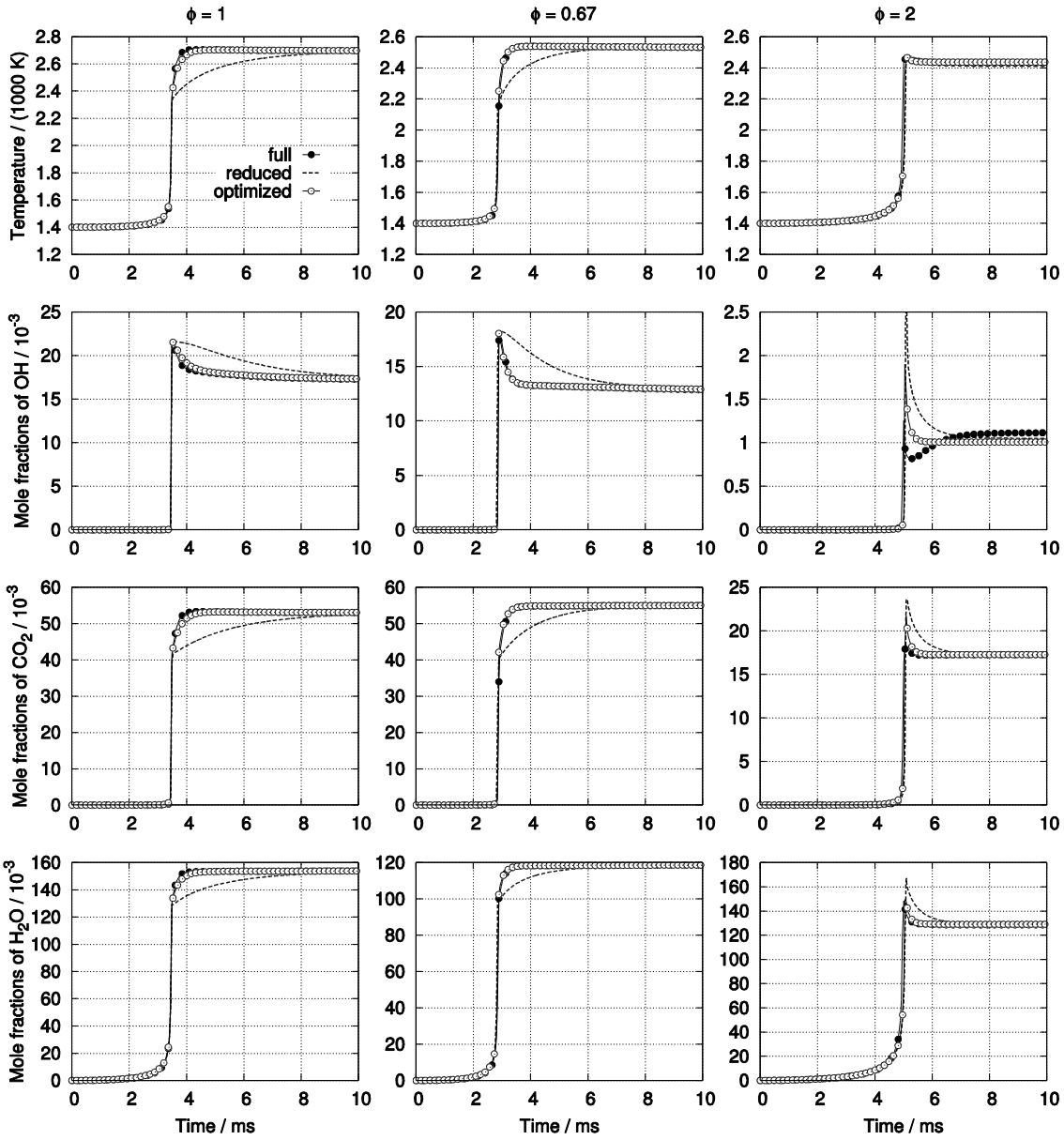

Figure 4 Auto ignition with the full, reduced, and optimized GRI-Mech 3.0 for p = 0.1 MPa, ϕ = 1 (left), ϕ = 0.67 (center), and ϕ = 2 (right).

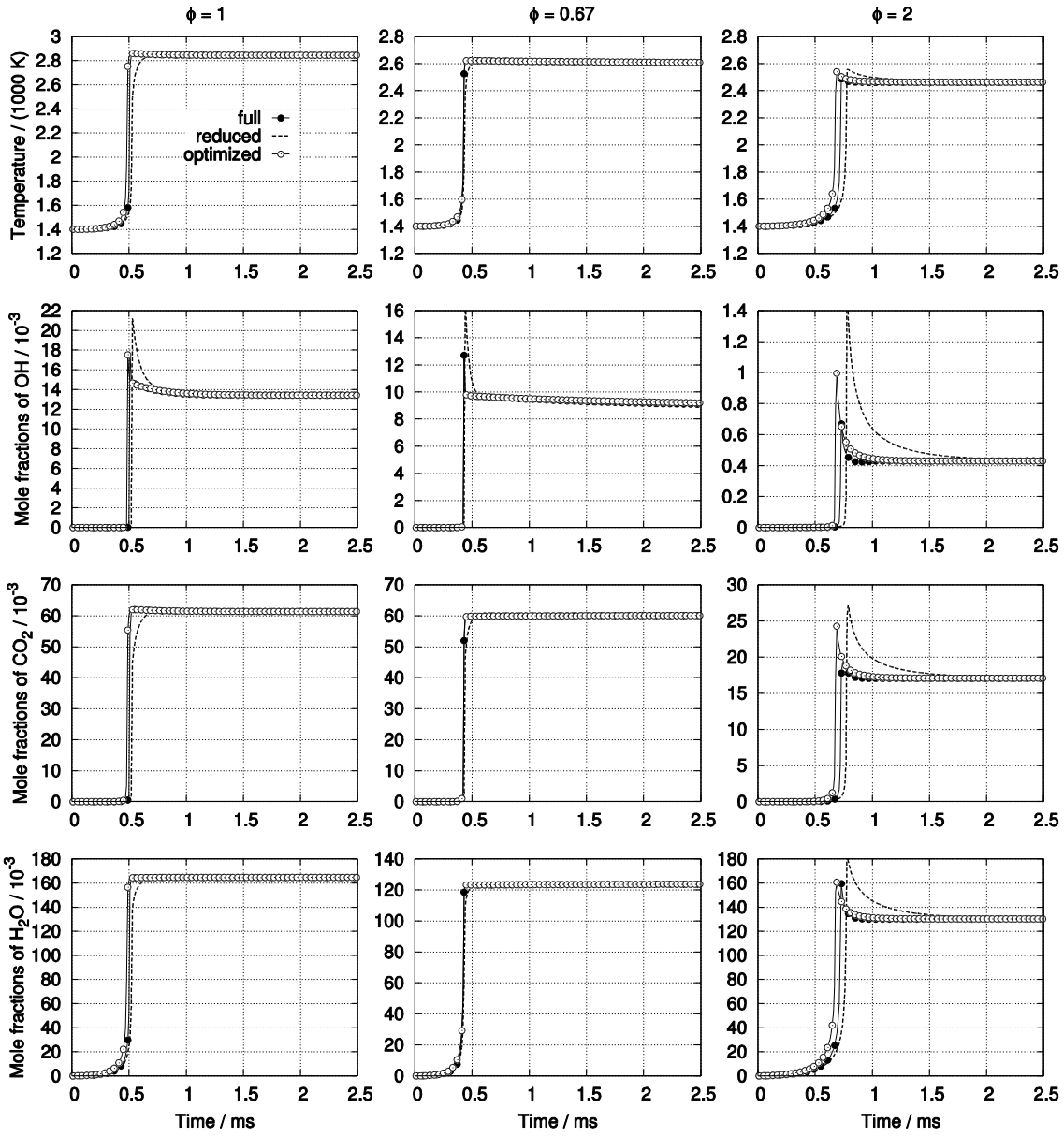

Figure 5 Auto ignition with the full, reduced, and optimized GRI-Mech 3.0 for p = 1 MPa, ϕ = 1 (left), ϕ = 0.67 (center), and ϕ = 2 (right).

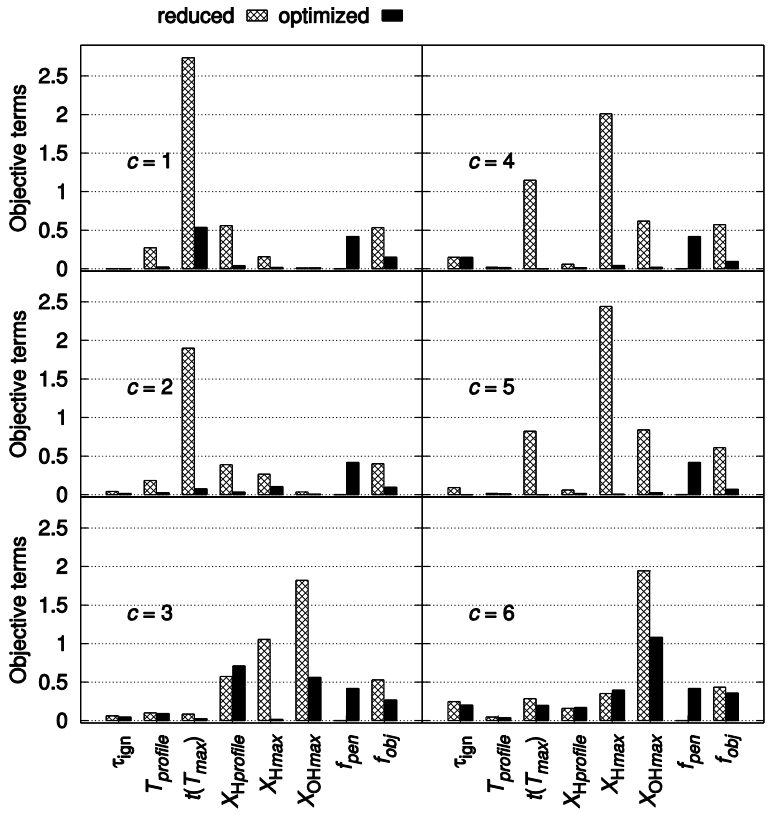

Figure 6 Values of single objective-function terms for conditions given in Table 1.

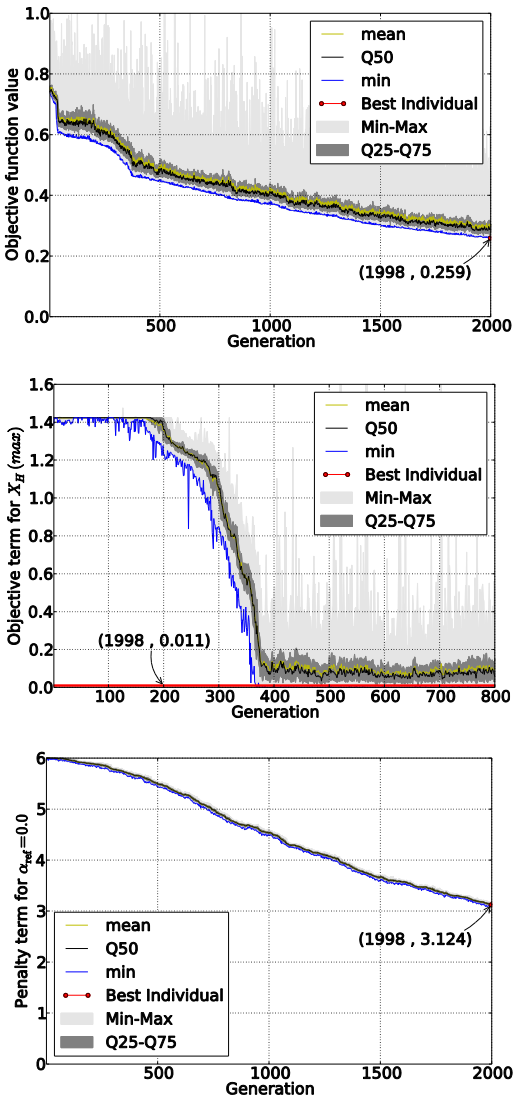

Figure 7 Evolution of: Overall objective function (top), the objective-function term $f_{H,max}$ (center) the penalty-function term (bottom) for the *tert*-butanol mechanism which lead to further elimination of 27 reactions.

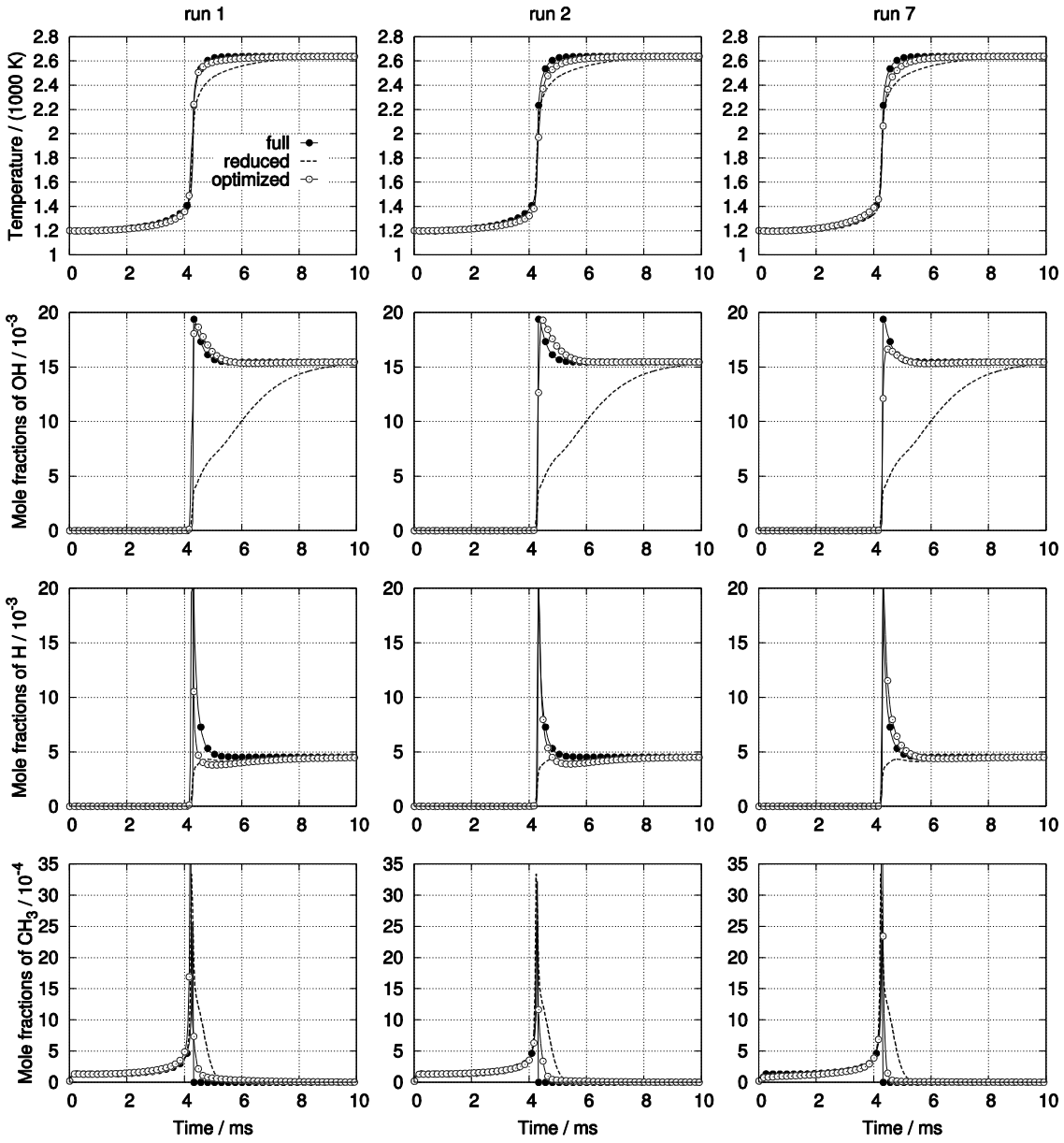

Figure 8 Auto ignition for full, reduced, and optimized *tert*-butanol mechanisms for a homogeneous constant-pressure reactor for runs 1, 2 and 7.

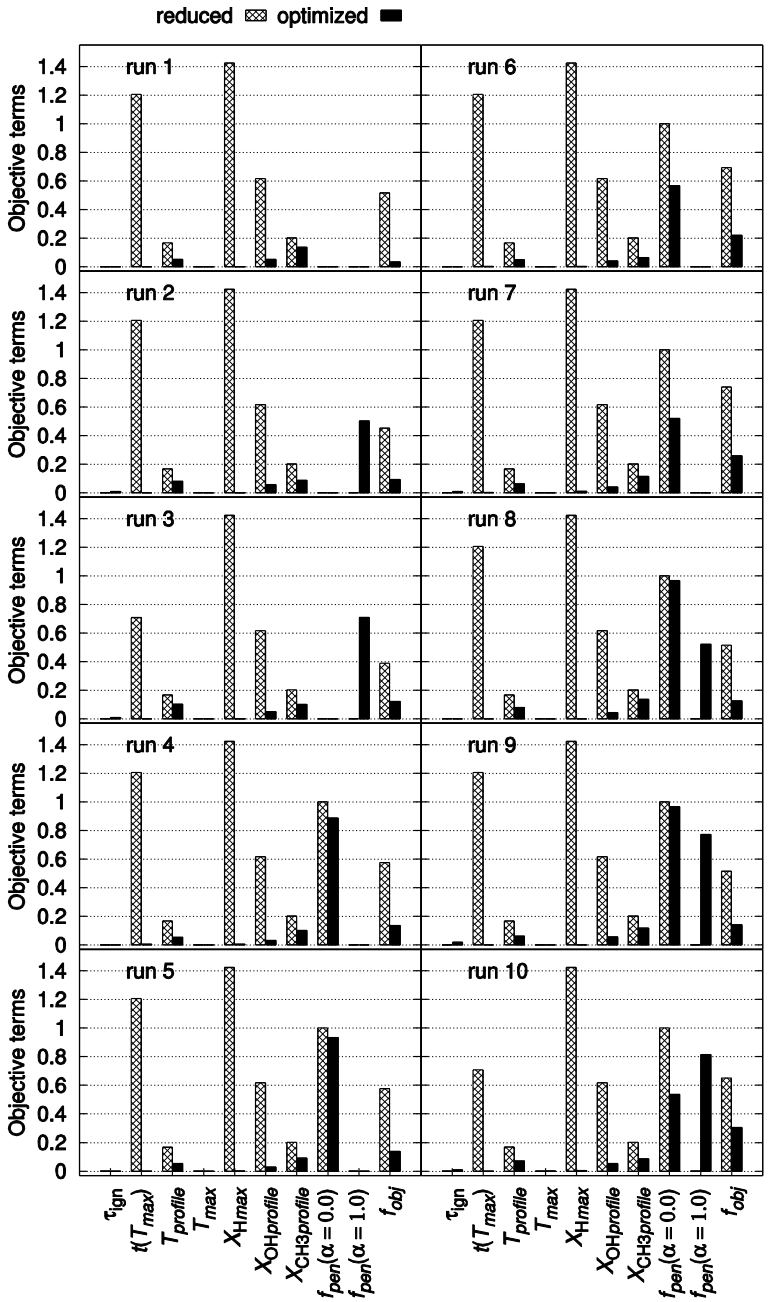

Figure 9 Values of single objective-function terms, before (reduced) and after the optimization (cf. Table 4).

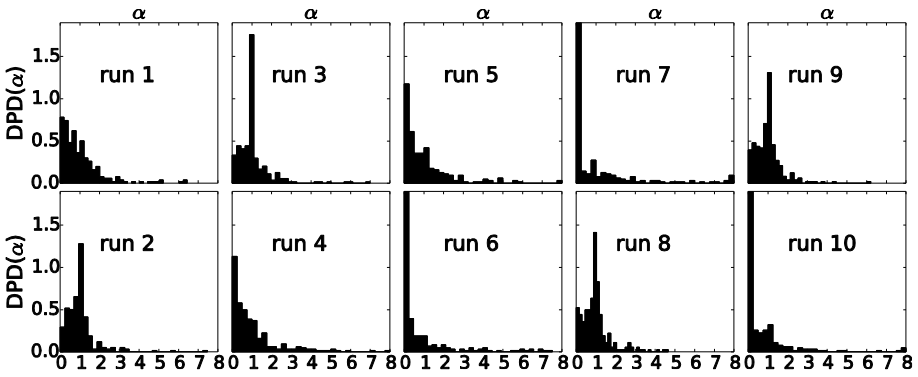

Figure 10 Discrete probability density of the normalized rate constants for the best individual from the *tert*-butanol mechanism optimization runs (cf. Table 4).

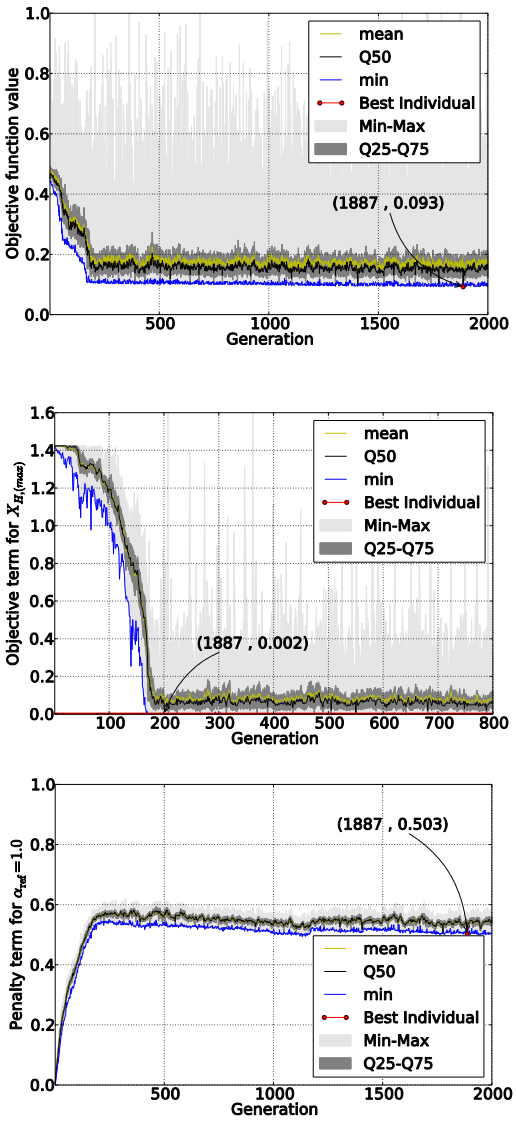

Figure 11 Evolution of the overall objective-function value (top), the objective-function term $f_{\mathrm{H,max}}$ (center), and the penalty-function term which constraints the change in rate coefficients (bottom) for run 2 (cf. Table 4).

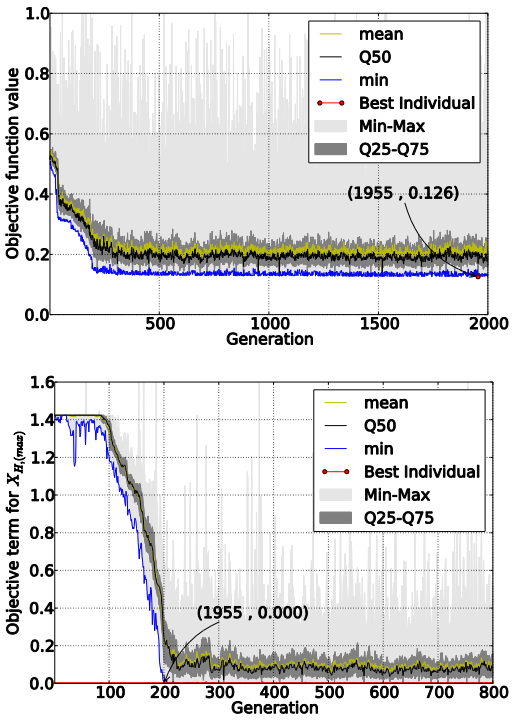

Figure 12 Evolution of the objective function value (top) and the objective-function term f_{Hmax} for run 8 (cf. Table 4).

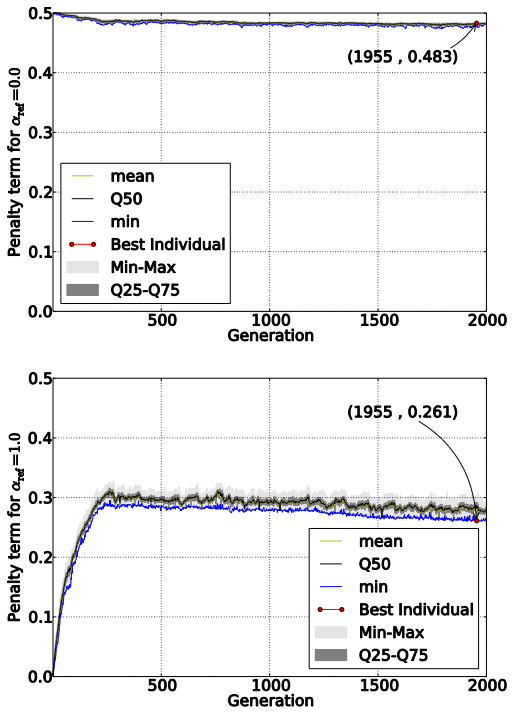

Figure 13 Evolution of the penalty-function term which drives the rate coefficients towards zero (top) to achieve a further reduction and the penalty-function term which constraints the change in rate coefficients for run 8 to maintain near original rate constants (cf. Table 4).

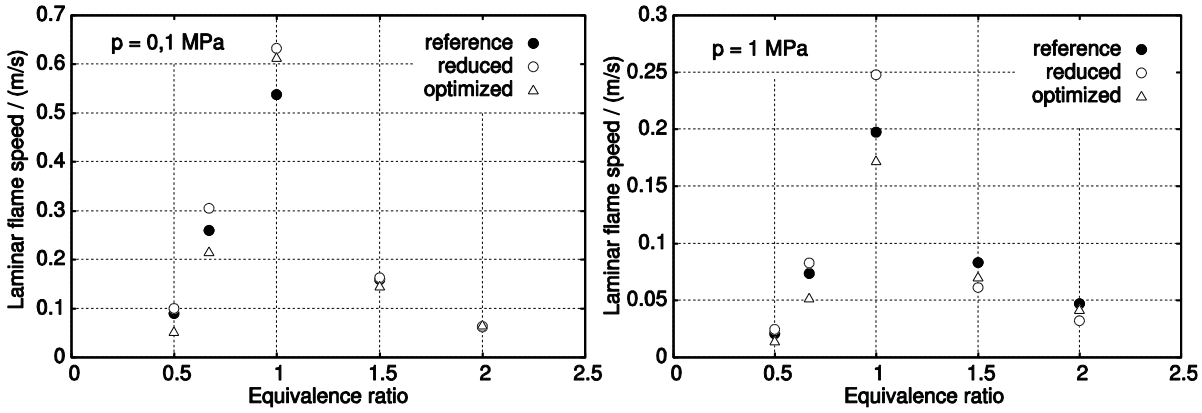

Figure A1 Laminar flame speed predictions for the full GRI 3.0 mechanism (reference) and the reduced and then optimized mechanisms as a function of equivalence ratio.

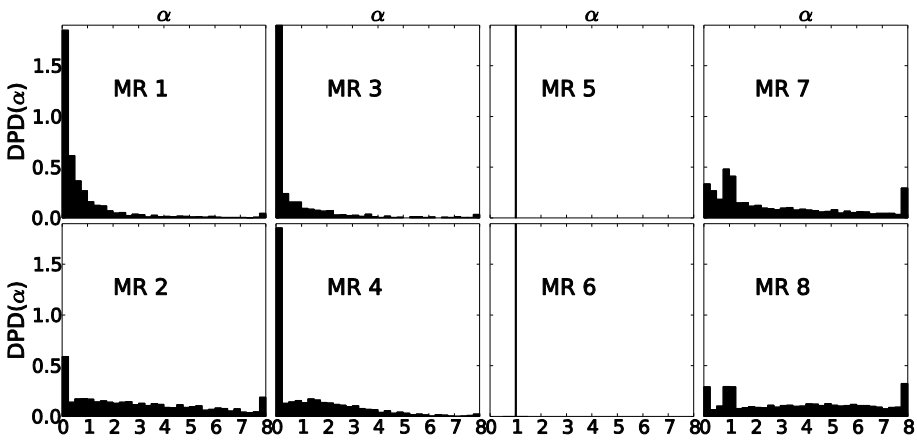

Figure B1 Different mutation types represented in terms of the discrete probability density of the normalized rate constants for the best individual, from the *tert*-butanol mechanism optimization runs without accuracy criteria.

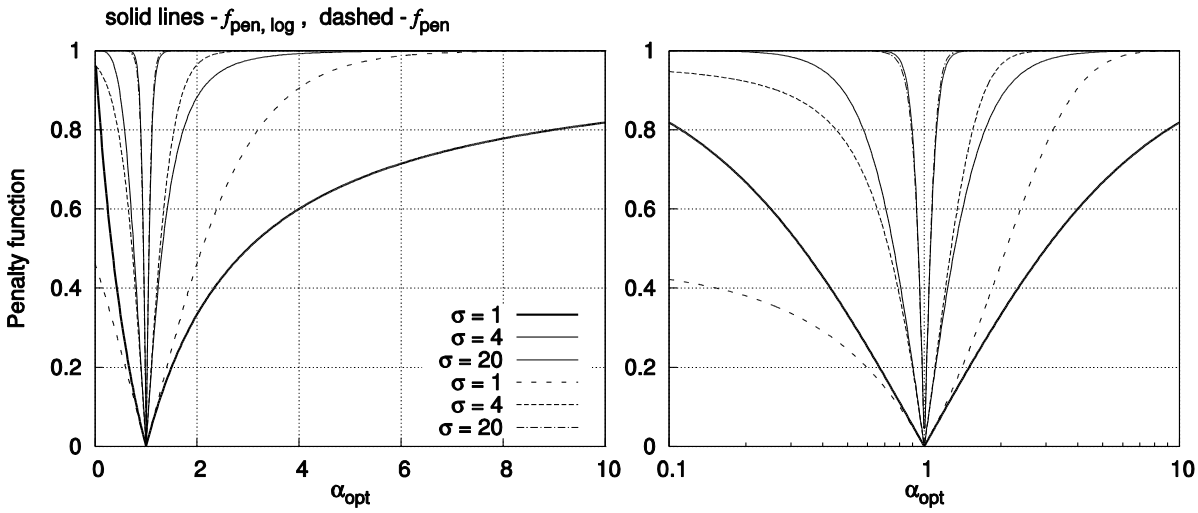

Figure C1 Comparison of the penalty functions from Eq. 7 and 8 in linear (left) and logarithmic (right) scale of the normalized rate constants.

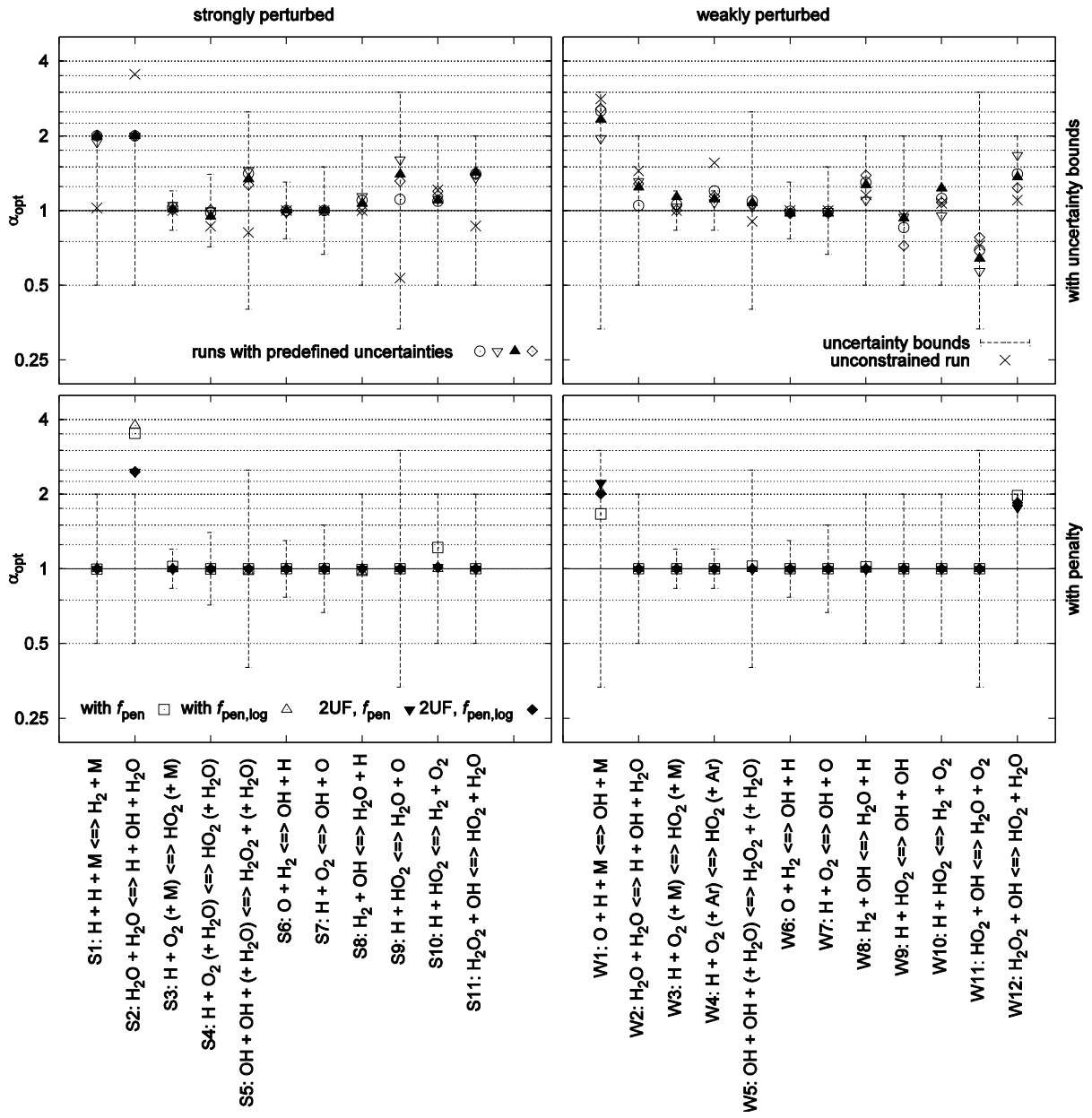

Figure D1 Extent of reaction rate modifications in comparison to their uncertainty bounds for optimization runs performed on two reduced mechanisms with different degrees of perturbation. Top shows the rate modifications resulting from one unconstrained and four UF-constrained runs.
Bottom shows the results from runs with penalty functions: with a penalty function f_{pen} only, with a logarithmic penalty function $f_{pen,log}$ only, with the uncertainty bounds defined with 2UF and penalty function f_{pen}, with the uncertainty bounds defined with 2UF and penalty function $f_{pen,log}$.
Left shows the optimization of a strongly perturbed (11 step) reduced mechanism, right shows the optimization of a weakly perturbed (12 step) reduced mechanism.

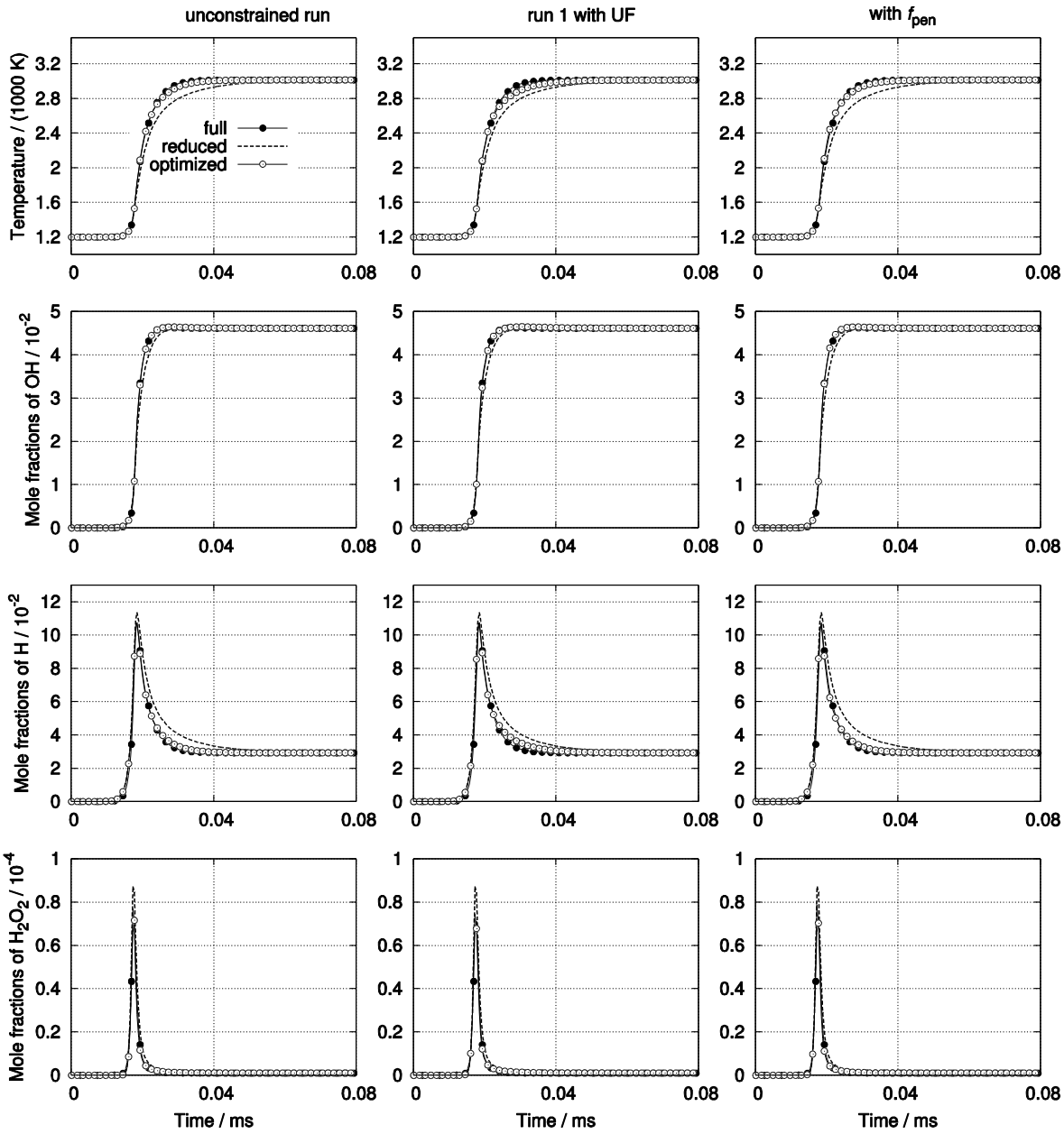

Figure D2 Auto ignition for full, reduced and optimized hydrogen mechanism resulting from three optimization runs with the same numerical setup and the accuracy criteria but different constraints imposed to reaction rate modifications: no constraints (left), with predefined uncertainty factor UF (center) and with penalty function $f_{pen}(\alpha_{ref} = 1.0)$ to minimize the modification (right).
The input mechanism was reduced with strong perturbation.

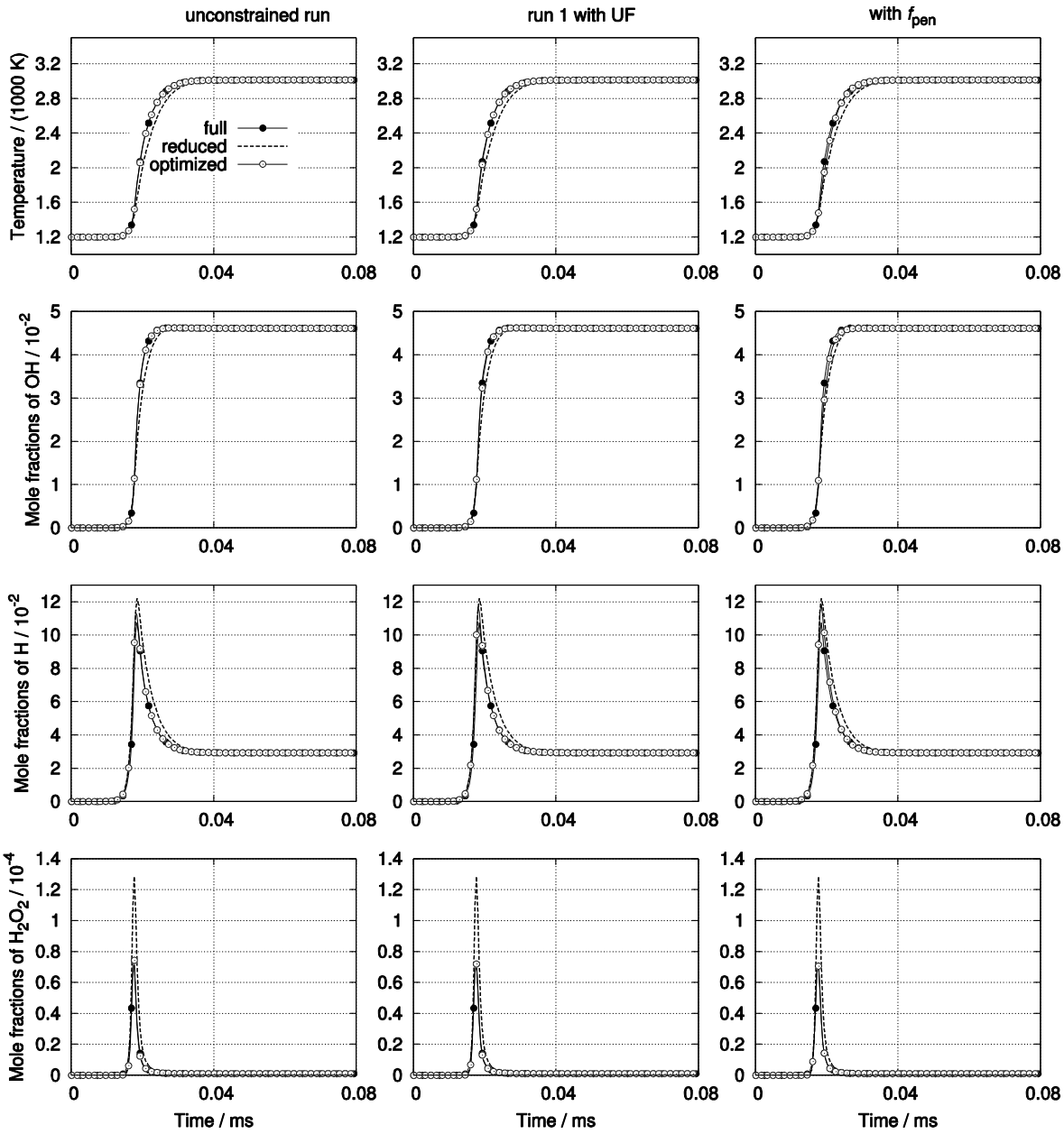

Figure D3 Auto ignition for full, reduced and optimized hydrogen mechanism resulting from three optimization runs with the same numerical setup and the accuracy criteria but different constraints imposed to reaction rate modifications: no constraints (left), with predefined uncertainty factor UF (center) and with penalty function $f_{pen}(\alpha_{ref} = 1.0)$ to minimize the modification (right).
The input mechanism was reduced with weak perturbation.

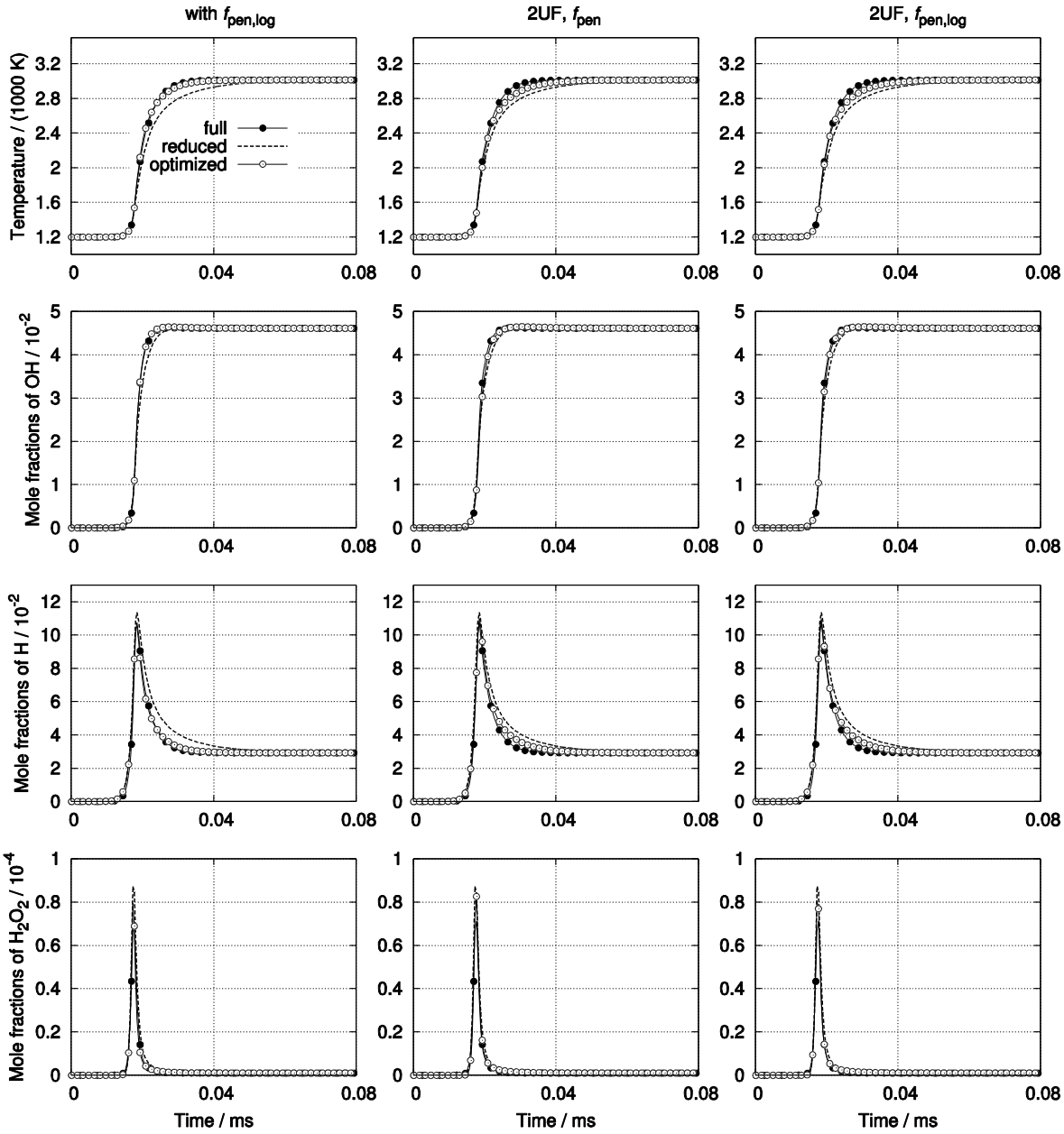

Figure D4 Auto ignition for full, reduced and optimized hydrogen mechanism resulting from three optimization runs with the same numerical setup and the accuracy criteria but different constraints imposed to reaction rate modifications: penalty function $f_{pen,log}$ (left), with doubled UF and f_{pen} (center) and with doubled UF and $f_{pen,log}$ (right).
The input mechanism was reduced with strong perturbation.

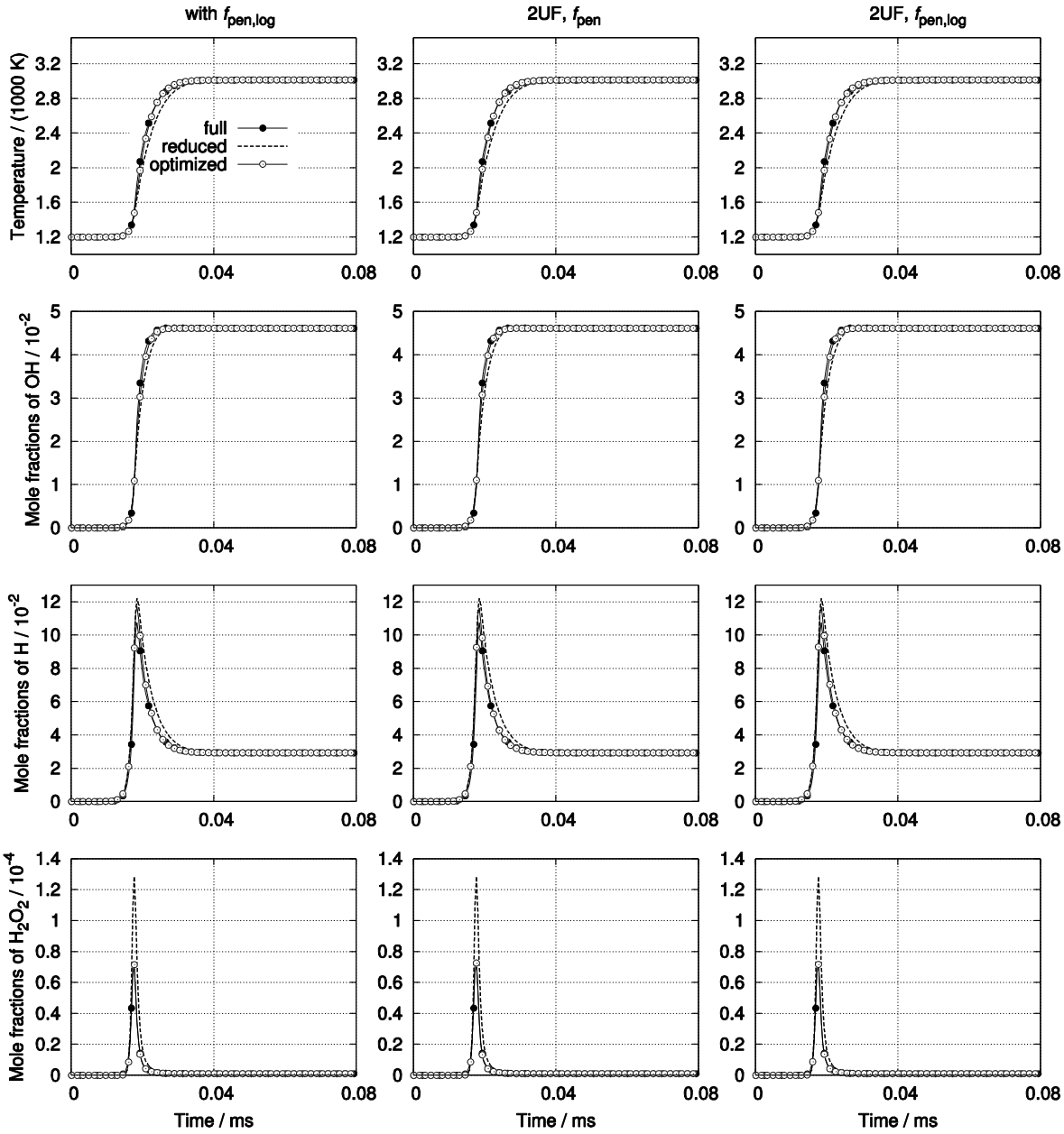

Figure D5 Auto ignition for full, reduced and optimized hydrogen mechanism resulting from three optimization runs with the same numerical setup and the accuracy criteria but different constraints imposed to reaction rate modifications: penalty function $f_{pen,log}$ (left), with doubled UF and f_{pen} (center) and with with doubled UF and $f_{pen,log}$ (right).
The input mechanism was reduced with weak perturbation.

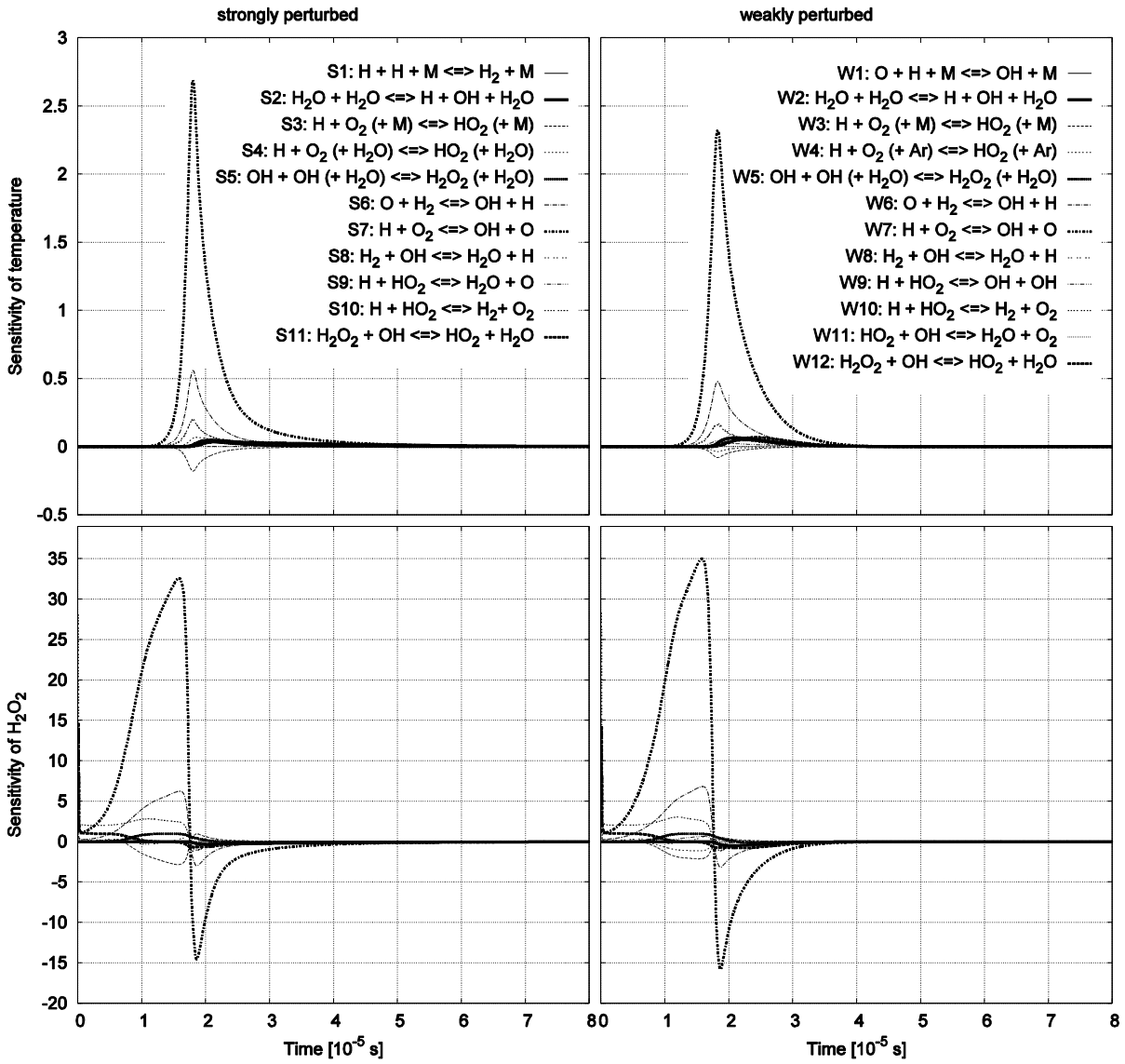

Figure D6 Normalized sensitivities of the temperature (top) and H_2O_2 (bottom) in respect to the remaining reactions in two reduced mechanisms.

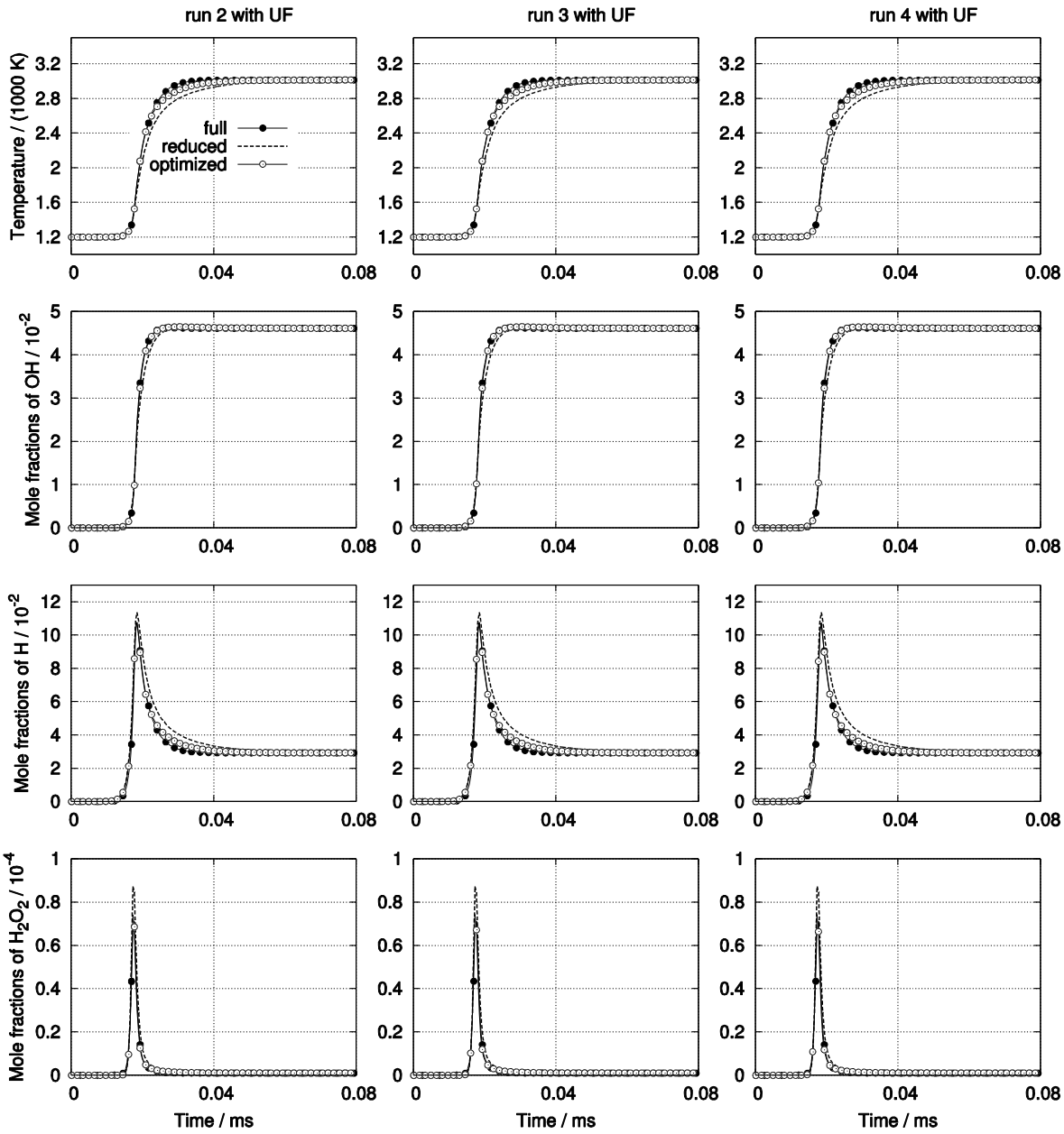

Figure D7 Auto ignition for full, reduced and optimized hydrogen mechanism resulting from three optimization runs with the same numerical setup, the accuracy criteria and predefined uncertainty factors UF. The input mechanism was reduced with strong perturbation.

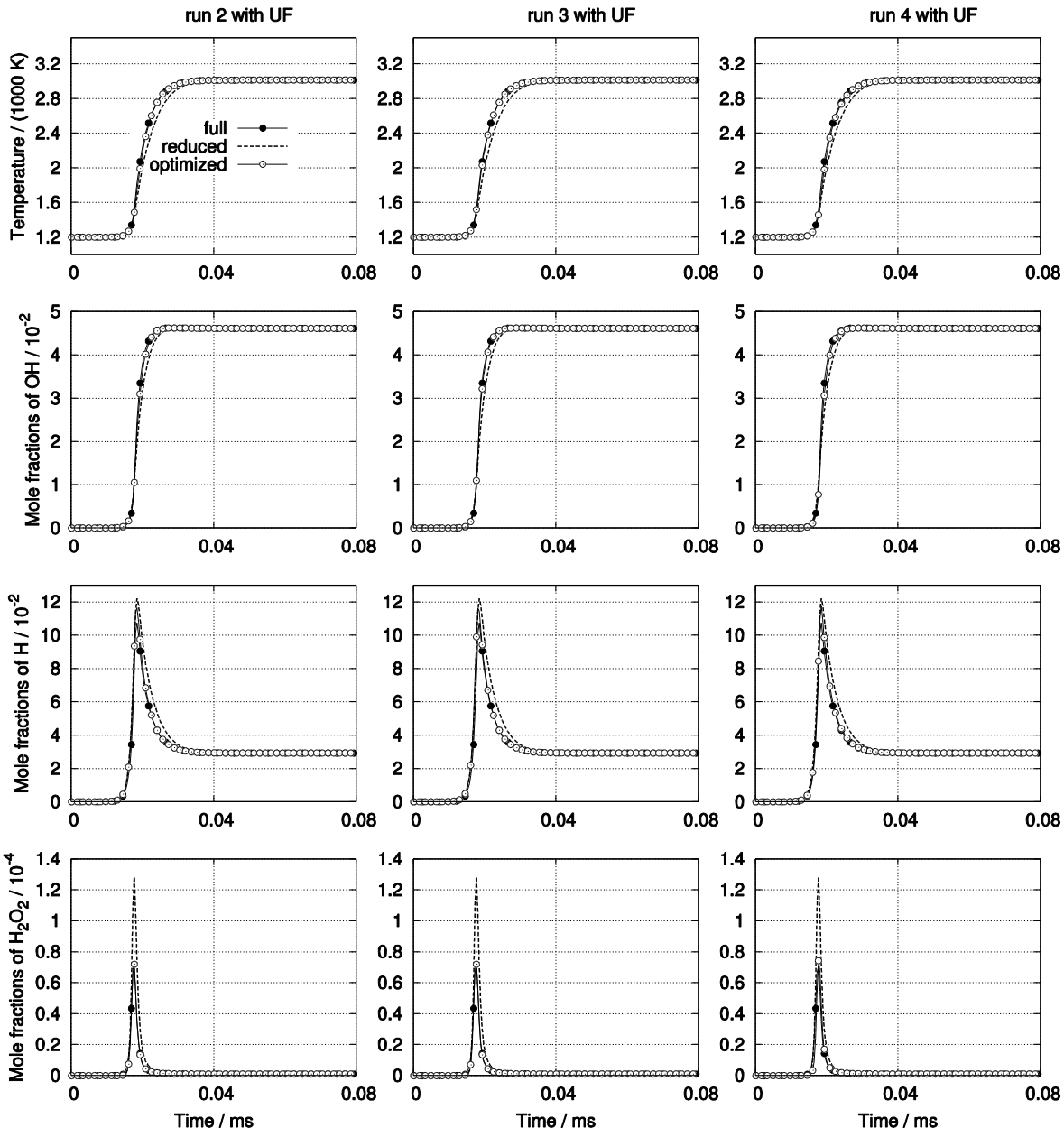

Figure D8 Auto ignition for full, reduced and optimized hydrogen mechanism resulting from three optimization runs with the same numerical setup, the accuracy criteria and predefined uncertainty factors UF. The input mechanism was reduced with weak perturbation.

Figure Captions

Figure 1 A uniform crossover between two parents

Figure 2 Logarithmic scaling of property ξ (a), sigmoid normalization (b) of a property ξ, and the penalty function $f_{\text{pen},i}$ where $\alpha_{i,\text{ref}} = 1.0$ (c). The penalty function for $\alpha_{i,\text{ref}} = 0.0$ is identical to that shown in (b).

Figure 3 Evolution of the objective function value for the methane/air mechanism optimization. Red line denotes the objective function value of the best individual which was found over 1000 generations.

Figure 4 Auto ignition with the full, reduced, and optimized GRI-Mech 3.0 for $p = 0.1$ MPa, $\phi = 1$ (left), $\phi = 0.67$ (center), and $\phi = 2$ (right).

Figure 5 Auto ignition with the full, reduced, and optimized GRI-Mech 3.0 for $p = 1$ MPa, $\phi = 1$ (left), $\phi = 0.67$ (center), and $\phi = 2$ (right).

Figure 6 Values of single objective-function terms for conditions given in Table 1.

Figure 7 Evolution of: Overall objective function (top), the objective-function term $f_{\text{H,max}}$ (center) the penalty-function term (bottom) for the *tert*-butanol mechanism which lead to further elimination of 27 reactions.

Figure 8 Auto ignition for full, reduced, and optimized *tert*-butanol mechanisms for a homogeneous constant-pressure reactor for runs 1, 2 and 7.

Figure 9 Values of single objective-function terms, before (reduced) and after the optimization (cf. Table 4).

Figure 10 Discrete probability density of the normalized rate constants for the best individual from the *tert*-butanol mechanism optimization runs (cf. Table 4).

Figure 11 Evolution of the overall objective-function value (top), the objective-function term $f_{\text{H,max}}$ (center), and the penalty-function term which constraints the change in rate coefficients (bottom) for run 2 (cf. Table 4).

Figure 12 Evolution of the objective function value (top) and the objective-function term f_{Hmax} for run 8 (cf. Table 4).

Figure 13 Evolution of the penalty-function term which drives the rate coefficients towards zero (top) to achieve a further reduction and the penalty-function term which constraints the change in rate coefficients for run 8 to maintain near original rate constants (cf. Table 4).

Figure A1 Laminar flame speed predictions for the full GRI 3.0 mechanism (reference) and the reduced and then optimized mechanisms as a function of equivalence ratio.

Figure B1 Different mutation types represented in terms of the discrete probability density of the normalized rate constants for the best individual, from the *tert*-butanol mechanism optimization runs without accuracy criteria.

Figure C1 Comparison of the penalty functions from Eq. 7 and 8 in linear (left) and logarithmic (right) scale of the normalized rate constants.

Figure D1 Extent of reaction rate modifications in comparison to their uncertainty bounds for optimization runs performed on two reduced mechanisms with different degrees of perturbation. Top shows the rate modifications resulting from one unconstrained and four UF-constrained runs.
Bottom shows the results from runs with penalty functions: with a penalty function f_{pen} only, with a logarithmic penalty function $f_{\text{pen,log}}$ only, with the uncertainty bounds defined with 2UF and penalty function f_{pen}, with the uncertainty bounds defined with 2UF and penalty function $f_{\text{pen,log}}$.
Left shows the optimization of a strongly perturbed (11 step) reduced mechanism, right shows the optimization of a weakly perturbed (12 step) reduced mechanism.

Figure D2 Auto ignition for full, reduced and optimized hydrogen mechanism resulting from three optimization runs with the same numerical setup and the accuracy criteria but different constraints imposed to reaction rate modifications: no constraints (left), with predefined uncertainty factor UF (center) and with penalty function $f_{\text{pen}}(\alpha_{\text{ref}} = 1.0)$ to minimize the modification (right).
The input mechanism was reduced with strong perturbation.

Figure D3 Auto ignition for full, reduced and optimized hydrogen mechanism resulting from three optimization runs with the same numerical setup and the accuracy criteria but different constraints imposed to reaction rate modifications: no constraints (left), with predefined uncertainty factor UF (center) and with penalty function $f_{pen}(\alpha_{ref} = 1.0)$ to minimize the modification (right).
The input mechanism was reduced with weak perturbation.

Figure D4 Auto ignition for full, reduced and optimized hydrogen mechanism resulting from three optimization runs with the same numerical setup and the accuracy criteria but different constraints imposed to reaction rate modifications: penalty function $f_{pen,log}$ (left), with doubled UF and f_{pen} (center) and with with doubled UF and $f_{pen,log}$ (right).
The input mechanism was reduced with strong perturbation.

Figure D5 Auto ignition for full, reduced and optimized hydrogen mechanism resulting from three optimization runs with the same numerical setup and the accuracy criteria but different constraints imposed to reaction rate modifications: penalty function $f_{pen,log}$ (left), with doubled UF and f_{pen} (center) and with with doubled UF and $f_{pen,log}$ (right).
The input mechanism was reduced with weak perturbation.

Figure D6 Normalized sensitivities of the temperature (top) and H_2O_2 (bottom) in respect to the remaining reactions in two reduced mechanisms.

Figure D7 Auto ignition for full, reduced and optimized hydrogen mechanism resulting from three optimization runs with the same numerical setup, the accuracy criteria and predefined uncertainty factors UF. The input mechanism was reduced with strong perturbation.

Figure D8 Auto ignition for full, reduced and optimized hydrogen mechanism resulting from three optimization runs with the same numerical setup, the accuracy criteria and predefined uncertainty factors UF. The input mechanism was reduced with weak perturbation.